

PWA FR-1716
4 FEB 1966

INVESTIGATION OF PRESSURE PREDICATION METHODS FOR LOW FLOW RADIAL IMPELLERS PHASE III FINAL REPORT



Prepared Under Contract NA58-5442
For
George C. Marshall Space Flight Center
Huntsville, Alabama

GPO PRICE \$ _____
CFSTI PRICE(S) \$ _____
Hard copy (HC) \$ 3.00
Microfiche (MF) \$ 1.75

653 JULY 65

FACILITY FORM 602	N66 21867	
	(ACCESSION NUMBER)	(THRU)
	178	1
	(PAGES)	
CR-71637		
(NASA CR OR TMX OR AD NUMBER)	(CATEGORY)	
		28

Pratt & Whitney Aircraft

FLORIDA RESEARCH AND DEVELOPMENT CENTER

DIVISION OF UNITED AIRCRAFT CORPORATION
**U
A.**

INVESTIGATION OF
PRESSURE PREDICATION METHODS
FOR LOW FLOW RADIAL IMPELLERS

PHASE III

FINAL REPORT



Prepared Under Contract NAS8-5442
For
George C. Marshall Space Flight Center
Huntsville, Alabama

Written By: W. E. Young and H. F. Due
W. E. Young H. F. Due
Program Manager Senior Engineer

Approved By: C. D. Lingenfelter
C. D. Lingenfelter
Project Engineer

Pratt & Whitney Aircraft
FLORIDA RESEARCH AND DEVELOPMENT CENTER

DIVISION OF UNITED AIRCRAFT CORPORATION



FOREWORD

This report was prepared by the Florida Research and Development Center of Pratt & Whitney Aircraft and presents a summary of the work conducted under Contract NAS8-5442, sponsored by the George C. Marshall Space Flight Center of the National Aeronautics and Space Administration, Huntsville, Alabama.

The pressure prediction program was administered under the technical direction of the Turbomachinery Unit of the Engine Systems Branch, Mr. Loren C. Gross, Chief. This work was conducted in three phases covering the period from June 1963 to February 1966. Summaries of the work completed in the first two phases of the contract were presented in PWA FR-952, "A Study of Pressure Prediction Methods for Radial Flow Impellers" covering the period from June 1963 to March 1964 (Phase I) and PWA FR-1276 "Investigation of Pressure Prediction Methods for Radial Flow Impellers" covering the period from March 1964 to February 1965 (Phase II).

ABSTRACT

This report presents the results of work performed under Contract NAS8-5442, "Pressure Prediction Methods for Low Flow Radial Impellers." The objectives of this program were to (1) determine, experimentally, the effect of changes in geometry and operating conditions on the radial pressure distribution along the low flow back face of centrifugal pump impellers, and (2) using the experimental results, formulate a computer program that can be used to predict pressure distribution within the range of variables tested. The work was conducted in three phases; the first phase was devoted exclusively to investigating incompressible flow performance with smooth and bladed disks in smooth housings using water as the test fluid. In the second phase the incompressible flow study was expanded to include rotor end effects and all previous tests were repeated to determine flow performance using liquid hydrogen as the test fluid. The third phase was intended to fill in and complete the data from the first two phases, and to investigate one additional configuration, that of a smooth disk with bladed housings.

The tests were conducted in an apparatus that consisted of a rotating disk enclosed in a stationary housing. The test fluid entered the apparatus at the eye of the disk on the front face and flowed radially outward to a collector or turnaround manifold at the tip. The flow was then directed radially inward down the back face to a discharge manifold located near the hub. This arrangement allows investigation of radially inward and outward flow conditions simultaneously.

Data recorded during each test included pressure measurements at the inlet, exit, and at several radial locations on both the front and back faces. The pressure data were used to develop regression equations for the fluid velocity ratio, K , (ratio of fluid angular velocity to wheel speed) for each configuration. These regression equations were then combined in a computer program written in Fortran II for use on the IBM 7090 computer. The computer program will determine the K value for a given configuration and set of operating conditions and then, applying this value to the forced vortex equation, compute the pressure distribution on the back face of the impeller.

CONTENTS

SECTION		PAGE
	ILLUSTRATIONS	v
	SYMBOLS	vii
I	INTRODUCTION	I-1
II	EXPERIMENTAL EQUIPMENT AND PROCEDURES	II-1
	A. Test Apparatus	II-1
	B. Test Facilities	II-1
	C. Instrumentation	II-4
	D. Test Configurations	II-7
	E. Experimental Procedure	II-8
III	EXPERIMENTAL RESULTS	III-1
	A. General	III-1
	B. Method of Analysis	III-1
	C. Discussion of Test Results	III-7
IV	DETERMINATION OF K VALUES	IV-1
V	DISCUSSION OF RESULTS	V-1
	A. General	V-1
	B. Formulation of Computer Program	V-3
VI	CONCLUSIONS	VI-1
VII	REFERENCES	VII-1
	APPENDIX A - Pressure Prediction for Radial Flow Impellers Fortran Program Formulation (PWA FRDC Deck No. 5363)	A-1

ILLUSTRATIONS

FIGURE		PAGE
II-1	Pressure Distribution Test Apparatus (1/4 Scale).	II-2
II-2	Schematic of Flow Loop for Water Tests	II-3
II-3	Schematic of Flow Loop for Liquid Hydrogen Tests.	II-3
II-4	Pressure Distribution Rig.	II-5
II-5	Liquid Hydrogen High Pressure Test Flow Loop . . .	II-6
II-6	Modified Pressure Distribution Test Apparatus. . .	II-6
II-7	View of Bladed Housings and Smooth Disk.	II-8
II-8	Pressure Distribution Test Apparatus	II-9
III-1	Radial Head Distribution for Smooth Disk in Water, Radially Outward Flow	III-5
III-2	Radial Head Distribution for Smooth Disk in Water, Radially Inward Flow.	III-6
III-3	Radial Head Distribution for Smooth Disk with Inlet Hub in Water, Radially Outward Flow.	III-8
III-4	Radial Head Distribution for Smooth Disk in Liquid Hydrogen, Radially Outward Flow	III-9
III-5	Radial Head Distribution for Smooth Disk in Liquid Hydrogen, Radially Inward Flow.	III-10
III-6	Radial Head Distribution for Bladed Disk in Water, Radially Outward Flow	III-11
III-7	Radial Head Distribution for Bladed Disk in Water, Radially Inward Flow.	III-12
III-8	Typical Radial Head Distribution for Bladed Disks in Liquid Hydrogen	III-13
III-9	Radial Head Distribution for Bladed Disk with Tip Blockage in Water.	III-14
III-10	Smooth Disk Torque Data.	III-16
III-11	Bladed Disk Torque Data.	III-16
III-12	Typical Panoramic Wave Analysis of Bladed Disk Test in Water.	III-19
III-13	Typical Peak-to-Peak Pressure vs Frequency	III-20
III-14	Blade Pressure Loading	III-21
III-15	Blade Pressure Loading vs Radius Ratio Squared for Bladed Disk in Liquid Hydrogen	III-22

ILLUSTRATIONS (Continued)

FIGURE		PAGE
IV-1	Fluid Velocity Ratio vs Flow Coefficient for Smooth Disk	IV-3
IV-2	Fluid Velocity Ratio vs Disk-to-Housing Clearance for Smooth Disk	IV-4
IV-3	Fluid Angular Velocity Correlation for 24-Blade, 0.250-in. Impeller in Water, Inward and Outward Flow.	IV-6
IV-4	Fluid Velocity Ratio vs Radius Ratio Squared for Bladed Disk in Liquid Hydrogen, Radially Inward Flow	IV-7
IV-5	Fluid Velocity Ratio vs Flow Coefficient for Smooth Disk with Inlet Hub, Radially Outward Flow.	IV-9
IV-6	Fluid Velocity Ratio vs Radius Ratio Squared for Bladed Disk with Tip Blockage in Water, Radially Outward Flow	IV-10
V-1	Temperature Rise for Outward Flow	V-2

SYMBOLS

Symbol	Nomenclature	Units
C	Axial clearance between rotor and housing	Inches
C_m	Torque coefficient, $M/1/2 \rho \omega_w^2 R_o^5$ where M is frictional torque (moment) for both sides of disk	Dimensionless
f()	Function of	
g	Acceleration due to gravity	ft/sec ²
H	Fluid static head	feet
K	Fluid angular velocity ratio, β/ω	Dimensionless
— _o	Subscript, o, referring to the outer edge of disk or impeller	
P	Static pressure (Absolute)	psia
Δp	Peak-to-peak pressure pulse at blade passing frequency	psi
R	Impeller or disk radius	feet
Re	Reynolds number of disk, $\omega R_o^2/\nu$	Dimensionless
S	Axial distance between housing and impeller surface, T + C	Inches
T	Blade height	Inches
u	Tangential impeller or disk velocity component	ft/sec
— _{1,2}	Subscripts referring to radial location on disk	
β	Angular velocity of fluid	rad/sec
γ	Specific weight of fluid	lb/ft ³
ν	Kinematic viscosity	ft ² /sec
ϕ	Flow coefficient at impeller tip, C_m/u	Dimensionless
ω	Angular velocity of impeller	rad/sec
z	Clearance between tip blockage spacers and impeller or disk	Inches

SECTION I
INTRODUCTION

In the early stages of development of centrifugal high-pressure liquid hydrogen and liquid oxygen turbopumps at Florida Research and Development Center, bearing failures were encountered due to unexpectedly high rotor axial thrust loads. These pumps were designed with thrust balance systems to carry predicted axial loads; however, data from early tests showed that pressures on the back faces of the impellers were not as predicted, resulting in axial forces 10 to 15% higher than anticipated. It was readily apparent that the existing methods for predicting pressure distribution on the back face of the impellers were not sufficiently accurate for high-pressure pump applications where the pressure-area product results in axial loads on the order of 300,000 pounds.

This experience led to the initiation of Contract NAS8-5442, "Investigation of Pressure Prediction Methods for Low Flow Radial Impellers," in June 1963. The objective of this program was to develop a method of predicting the distribution of pressure on the back face of centrifugal impellers with greater accuracy than previously possible. The approach was to experimentally establish the effect on fluid angular velocity (β), as expressed by the relationship $\beta = K\omega$, of various impeller back face configurations and operating conditions. This was accomplished by measuring pressures along the front and rear faces of the disk and using the data to calculate the value of K from the forced vortex equation.

$$P_2 - P_1 = \left(\gamma K^2 \omega^2 / 2g \right) \left(R_2^2 - R_1^2 \right)$$

Regression equations for K were then formulated for each configuration using a statistical fit of the test data. These equations reflect the dependence of K on each variable.

Three basic rotor-housing configurations were investigated in the program representing three distinct levels of fluid angular velocity and, therefore, pressure distribution. The three configurations were (1) a bladed disk with smooth housings, which provides high fluid velocities, (2) a smooth (unbladed) disk with smooth housings, which provides moderate velocities, and (3) a smooth disk with bladed housings, which produces little or no fluid rotation.

The effects of changes in disk inlet and discharge geometry were also investigated by adding an inlet hub to the smooth disk and blockage rings that simulate casing overhang at the tip of the bladed disk.

Each configuration was tested over a range of disk-to-housing clearances, disk speed and flowrate in a test apparatus designed specifically for this program.

The regression equations for K developed from the test data were subsequently combined in a computer program written in Fortran II for use on the IBM 7090 computer. This program is capable of predicting pressure distribution on the low flow back face of centrifugal pump impellers more accurately than previous design systems for the range of variables investigated.

SECTION II
EXPERIMENTAL EQUIPMENT AND PROCEDURES

A. TEST APPARATUS

The test apparatus (figure II-1) consists of three large stainless steel housings that enclose an 11-inch diameter disk. The overhung disk is supported by two shaft bearings that are cooled by the test fluid during testing. Bearing lubrication is provided by the ball retainers. The bearings are mounted in a separate housing that also supports the main shaft seal. A smaller rear housing contains a purge cavity and secondary shaft seals, and adapts the test apparatus to the facility drive unit.

The disk-to-housing clearance can be adjusted with spacers between the front and rear main housings and between the flanges of the rear housing and the bearing housing.

The test fluid enters the apparatus through the front housing and flows radially outward along the disk to the collector ring at the tip formed by the intermediate housing. The flow is then directed radially inward along the back face of the disk to the discharge manifold located in the rear housing. Part of the flow is diverted through the bearings and out the bearing drain lines.

B. TEST FACILITIES

The experimental portion of the pressure prediction program was conducted in the FRDC rocket engine component test area. This area contains numerous test stands used for the testing of pumps, turbines, thrust chambers, bearings, and seals. All but one of the tests were conducted on test stand B-33, which is equipped with a 1500-hp constant-speed motor and a Dynamatic clutch and gearbox with a maximum output speed of 35,000 rpm. Speed can be controlled to within 1% of the set value. Schematics of the water and liquid hydrogen flow loops for B-33 stand are shown in figures II-2 and II-3, respectively. The water loop, which was a closed system, consisted of a 5000-gallon portable supply tank, a centrifugal boost pump, a filter, a turbine flowmeter, and a flow control valve. Demineralized water was used at a supply pressure of 90 psia and flowrates to 52 gpm.

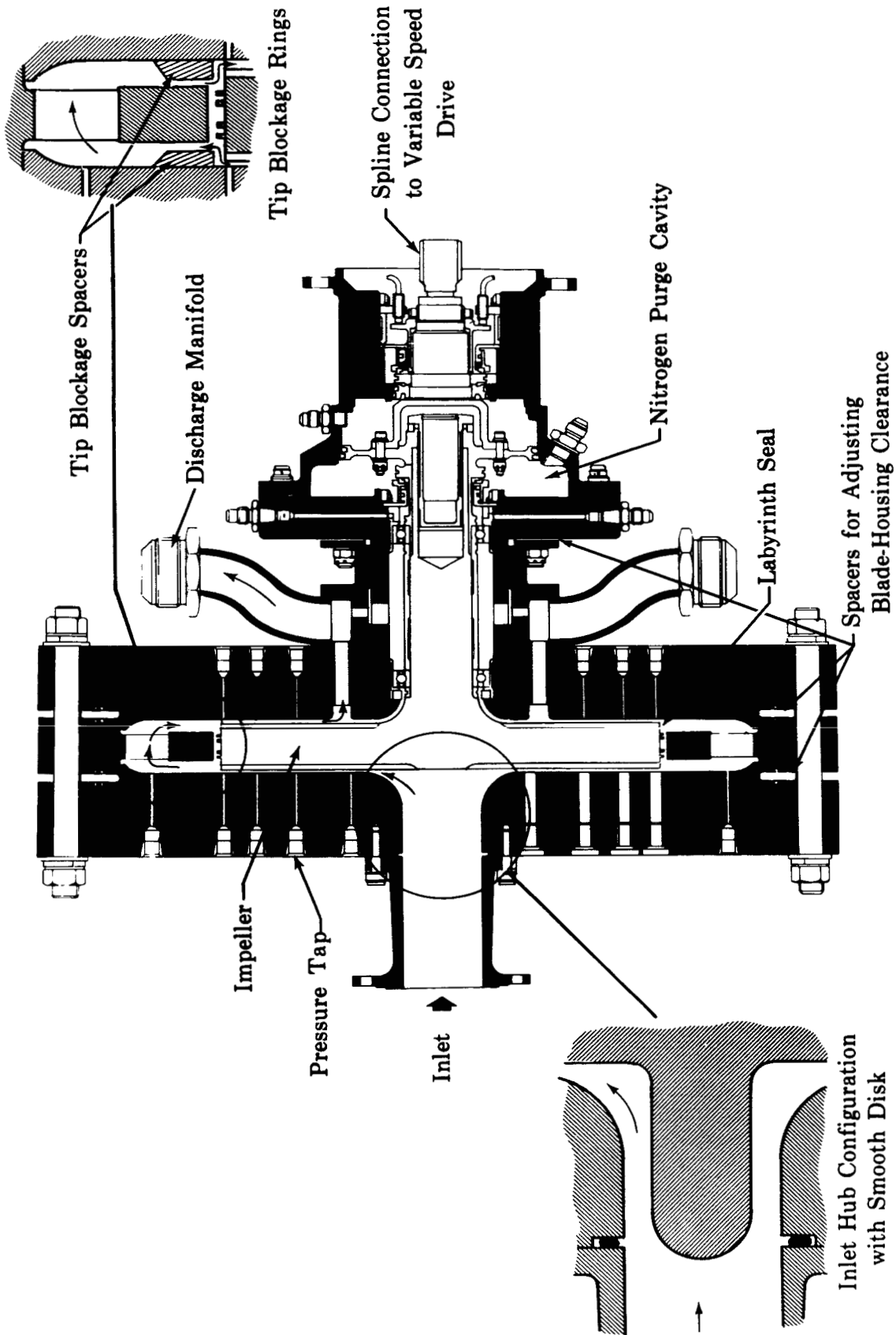


Figure II-1. Pressure Distribution Test Apparatus (1/4 Scale)

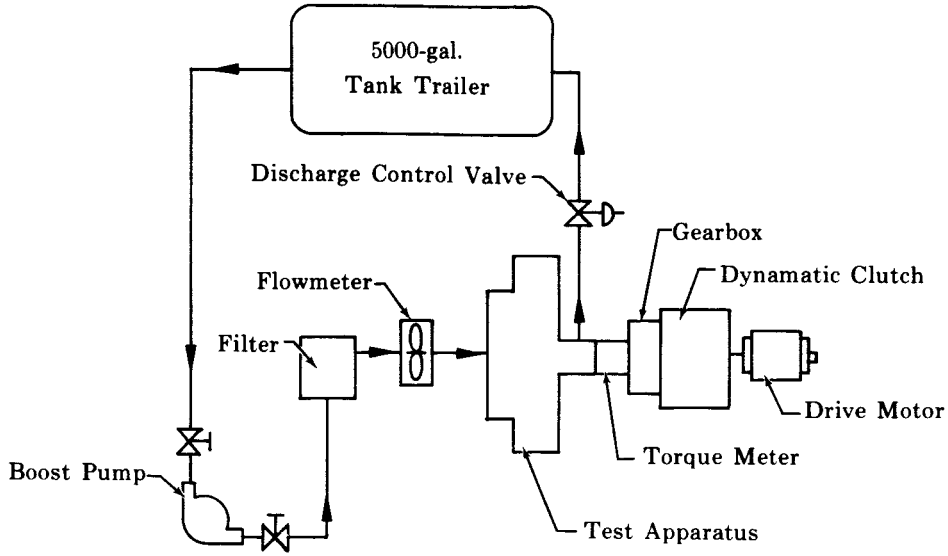


Figure II-2. Schematic of Flow Loop for Water Tests FD 11007

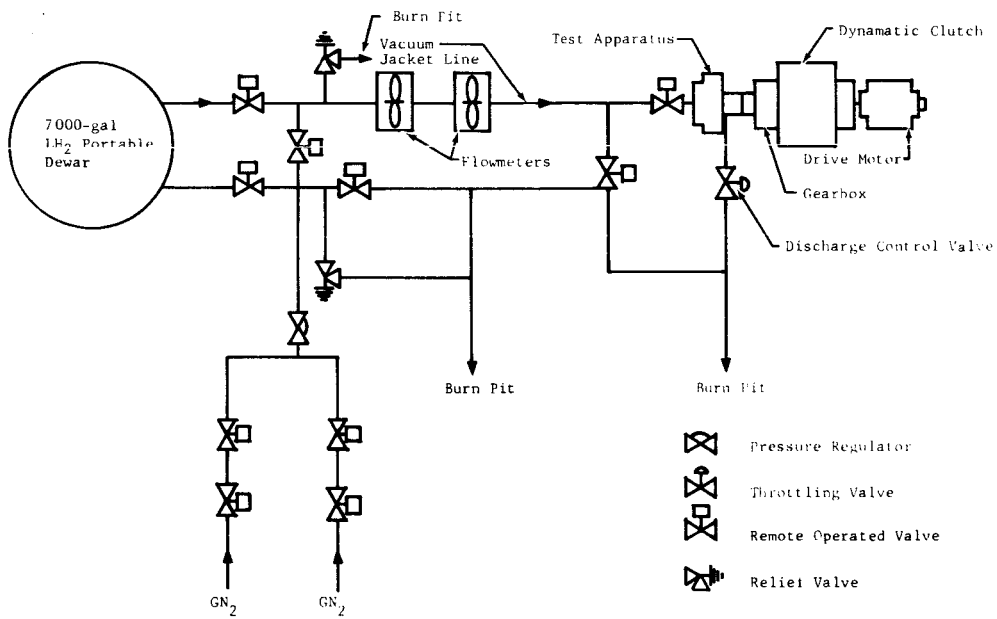


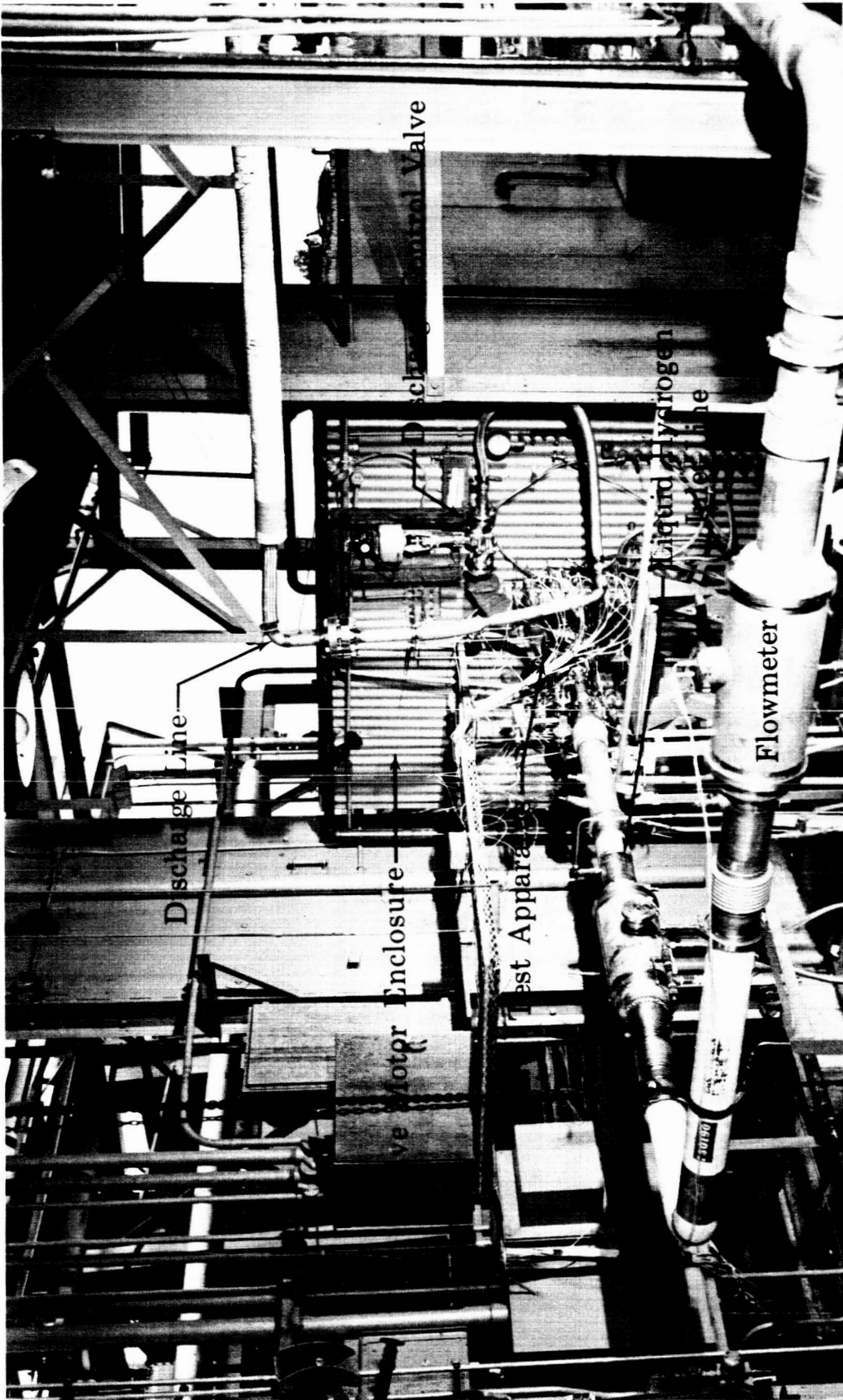
Figure II-3. Schematic of Flow Loop for Liquid Hydrogen Tests FD 14557

The hydrogen loop was an open system supplied by a 7000-gallon roadable dewar pressurized with gaseous hydrogen to approximately 90 psia. Liquid hydrogen passed through the vacuum-jacketed inlet line and flowmeters to the test rig and was then discharged through a control valve to the burnstack. Gaseous hydrogen and nitrogen were provided for purging the stand system and the test apparatus. The test apparatus mounted in B-33 stand is illustrated in figure II-4.

One test during the third phase of the contract was conducted at an inlet pressure of approximately 650 psia, which was beyond the capability of the supply system in B-33 stand; therefore, this test was conducted in B-32 stand, which was constructed for high-pressure rocket engine component testing. This stand is equipped with two, 100-gallon, 550-psia supply tanks. A 5000-gallon roadable dewar was used to fill the supply tanks for cooldown of the stand plumbing and test apparatus. After cooldown the tanks are pressurized to the required inlet pressure and the run valve opened. As on B-33 stand, flowrate is regulated by a discharge control valve. Figure II-5 shows a schematic of the B-32 flow loop. B-32 stand does not have a drive system of sufficient power for this test apparatus; therefore, the test apparatus was modified (figure II-6) to incorporate a turbine drive unit similar to that used in the RL10 engine. The turbine was driven by a gaseous hydrogen blowdown system with a closed loop speed control. The discharge from both the turbine and the test apparatus was ducted to burnstacks for disposal.

C. INSTRUMENTATION

The instrumentation in the test apparatus was essentially the same for the water and hydrogen tests with the exception of the temperature sensors. Temperature measurements in liquid hydrogen were made with Rosemount resistance-type thermometers, Model No. 150 E and 157 T. Copper-constantan thermocouples were used in the water tests. Static pressures were measured at the inlet, discharge, and at the disk tip, plus four radial stations on the front housing and three radial stations on the rear. The pressure taps were close coupled with Tabor pressure transducers, Model 2175A.



FD 10993

Figure II-4. Pressure Distribution Rig

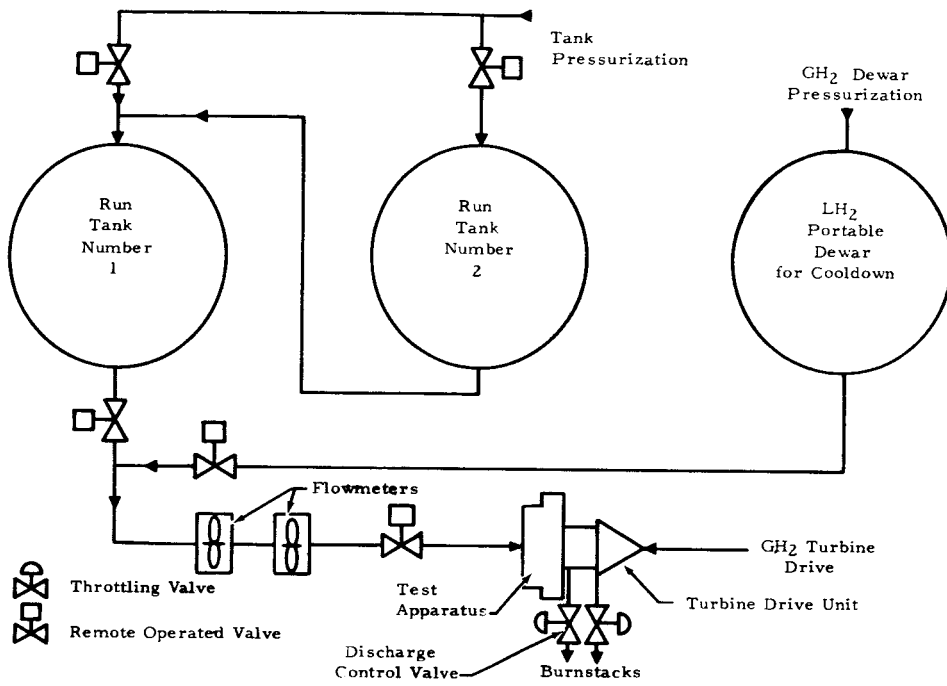


Figure II-5. Liquid Hydrogen High Pressure Test Flow Loop

FD 14558

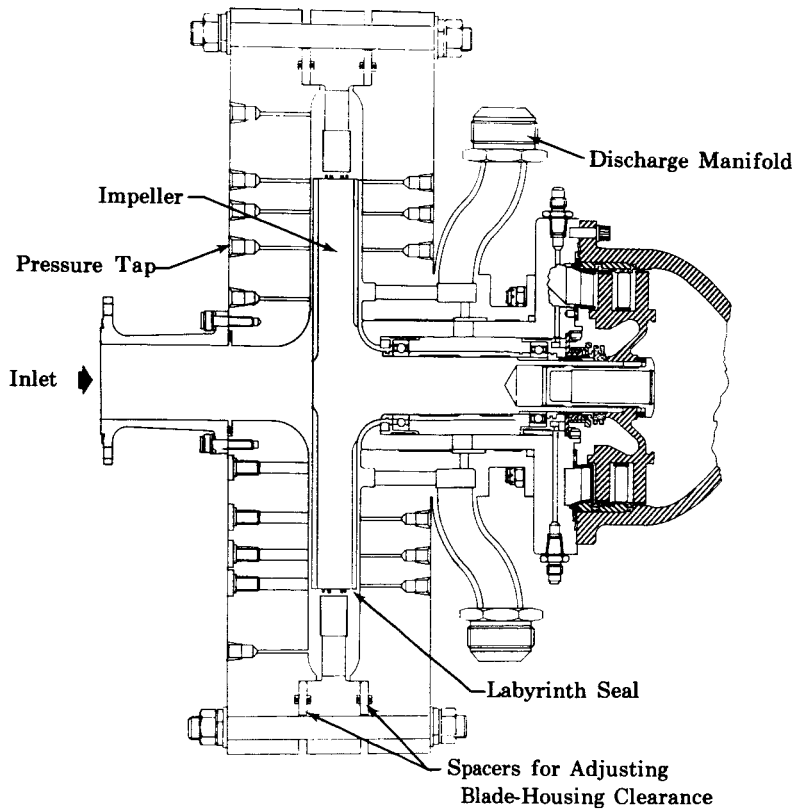


Figure II-6. Modified Pressure Distribution Test Apparatus

FD 10984B

Pressure fluctuations generated by the rotating blades were measured during some of the bladed disk tests with Kistler Model 601A quartz crystal pressure transducers close coupled with Model 624 adapters. The data were recorded on a frequency-modulated tape unit and analyzed with a panoramic wave analyzer having a Polaroid attachment.

Temperature, pressure, flowrate, and speed data were recorded by an automatic data recording system on digital tape. Each data channel was scanned and recorded approximately every 0.014 sec.

A torque measuring device, consisting of a torque sensor shaft using gears and magnetic pickups located at each end, was used in the initial testing. The change in phase angle between the gear teeth as measured by the magnetic pickups indicated the angle of twist of the shaft, which in turn is proportional to the torque applied by the rotor.

D. TEST CONFIGURATIONS

Three basic impeller back face configurations were tested in this program: (1) a smooth disk in a smooth housing, (2) a bladed disk in a smooth housing, and (3) a smooth disk in a bladed housing. A more detailed description of each configuration is presented in the following paragraphs.

1. Smooth Disk and Smooth Housing

The smooth unbladed disk was tested over a range of disk-to-smooth housing clearances from 0.024 to 0.138 in. Tests were also conducted with an inlet hub added to the disk as shown in the insert on figure II-1. Two hub sizes, which produced inlet diameter-to-hub diameter ratios of 1.33 and 2.00, were included.

2. Bladed Disk and Smooth Housing

The bladed disk configurations and the clearances at which they were tested are as follows: In this series of tests the number of blades was also varied.

No. of Blades	Blade Height, in.	Clearance, in.
24	0.125	0.020 - 0.135
24	0.250	0.024 - 0.140
12	0.125	0.067 - 0.074
6	0.125	0.067 - 0.075

The 24 - 0.125-inch bladed disk was also tested with tip blockage rings that simulated housing overhang, (see insert figure II-1). Three disk-to-blockage ring clearances (0.050, 0.100, and 0.150 in.) were tested at various blade-to-housing clearances.

3. Smooth Disk and Bladed Housing

For this configuration 12 - 0.135-in. high blades were welded to the front and rear housings as shown in figure II-7. The bladed housings were tested with a smooth disk at clearances from 0.038 to 0.128 inch.

E. EXPERIMENTAL PROCEDURE

The test apparatus was assembled for each new disk and/or housing configuration with new ball bearings. Fits on critical components and runouts on the rotating assembly were checked. Most of the pressure transducers were mounted on the test apparatus, as shown in figure II-8, to facilitate changes in the disk-to-housing clearance that were made in the test stand and to reduce stand mounting time.

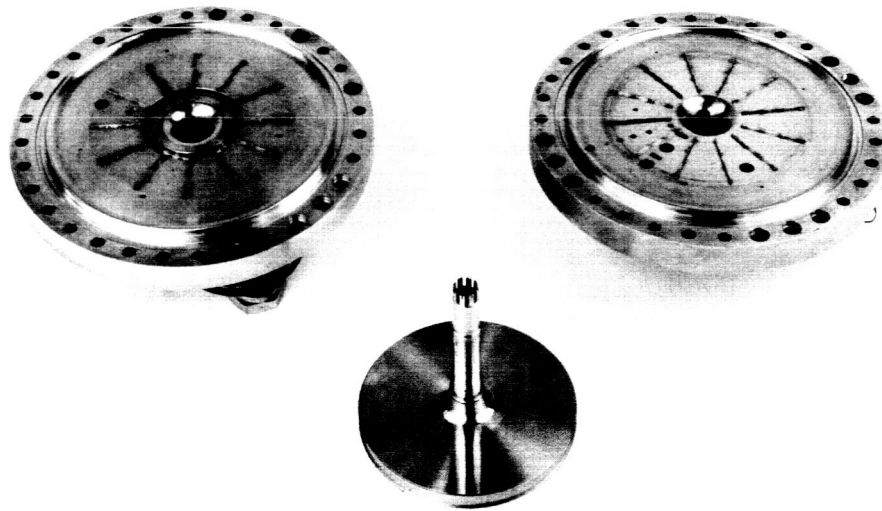


Figure II-7. View of Bladed Housings and Smooth Disk

FE 53902

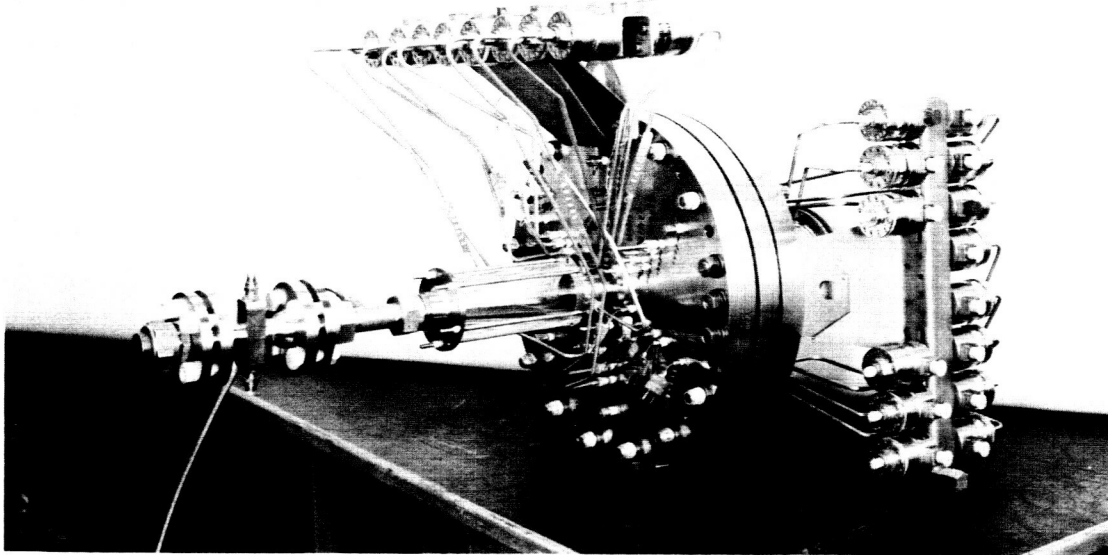


Figure II-8. Pressure Distribution Test
Apparatus

FE 37060

Each test was of approximately 20 minutes duration during which time up to 9 data points were recorded. Approximately 10 seconds of high-speed data were recorded during a period of several minutes of steady-state running at selected speeds and flowrates. Because of inherently different physical and thermodynamic properties of water and liquid hydrogen, the speed-flow limits were significantly different for the two fluids. The drive system torque limits (approximately 200 ft-lb) restricted the water tests to speeds up to 5000 rpm, and the supply pump output restricted flowrates to 50 gpm or less; however, this combination satisfactorily covered the range of flow coefficients required. Heat addition (due to fluid friction) limited the maximum speed in the hydrogen tests to approximately 14,000 rpm because of the tendency of the hydrogen to boil. The maximum hydrogen flowrate was restricted to approximately 300 gpm by the pressure limit (90 psig) on the supply dewar. At the upper speed range the minimum flowrate was critical because of the energy input to the fluid. Cavitation within the test apparatus was noted when operating outside of these speed and flow limits. These limitations restricted the liquid hydrogen tests to flow coefficients between 0.015

and 0.030 (calculated at the disk tip); however, the data obtained were considered adequate to correlate the variables involved.

The data as received from the automatic data recording system were reduced to engineering units on the IBM 7090 computer immediately following each test run. The basic data, which consisted of pressures, temperatures, speeds, and flowrates, were then input to a data analysis program. The liquid hydrogen data analysis was performed on the IBM 7090 computer. The water data analysis was performed on the smaller IBM 1620 computer because of the fewer computations required. Data analysis output included such quantities as head rise, K values, Reynolds number, and flow coefficient.

SECTION III
EXPERIMENTAL RESULTS

A. GENERAL

The experimental results were obtained primarily in the form of head rise distribution (ΔH vs R^2) curves for the radially outward and inward flow conditions for each configuration. Head rise values, in feet of fluid, were obtained using the density as a function of the measured pressures and temperatures corresponding to the various radial locations along the disk. Table III-1 summarizes all of the test runs for Phases I, II, and III. This table gives the test fluids, axial blade tip-to-housing clearance, blade height, number of blades, and additional information. The range of variables for each test run included three levels of speed and three levels of flowrate.

A discussion of the method of analysis of the data and the results of the tests on each basic configuration, i.e., smooth disk, bladed disk, and bladed housing/smooth disk, are presented in the following paragraphs.

B. METHOD OF ANALYSIS

As a fluid is forced into rotation by an object that is performing external work on the fluid, such as a rotating disk (free or enclosed), a condition of equilibrium exists for each fluid particle. The condition of equilibrium requires that the centrifugal force must be balanced by the static pressure at the fluid particle. Considering an annular ring of fluid with a differential radius dR , the static pressure distribution is given by:

$$\int dP = \int \frac{\gamma}{g} \beta^2 R dR \quad (\text{III-1})$$

This equation shows the dependence of the static pressure distribution on the fluid density (γ) and the fluid angular velocity, β . In most cases the variation of γ with radius is small enough to neglect. The fluid angular velocity, however, has been shown to be a function of radius when factors such as flow and geometric variables are considered. If the variation of fluid angular velocity with radius is known, substitutions of this function into equation III-1 will permit the equation to be integrated to obtain the desired pressure distribution.

Table III-1. Summary of Tests

Test Phase	Test No.	Test Fluid	Axial Clearance, in.	Blade Height, in.	Number of Blades	Remarks
I	1	water	0.125	0	0	Smooth Disk
I	2	water	0.084	0	0	Smooth Disk
I	3	water	0.040	0	0	Smooth Disk
I	4	water	0.125	0.125	24	Bladed Disk
I	5	water	0.063	0.125	24	Bladed Disk
I	6	water	0.020	0.125	24	Bladed Disk
I	7	water	0.122	0.250	24	Bladed Disk
I	8	water	0.067	0.250	24	Bladed Disk
I	9	water	0.024	0.250	24	Bladed Disk
I	10	water	0.067	0.125	12	Bladed Disk
I	11	water	0.067	0.125	6	Bladed Disk
II	12	water	0.080	0	0	Smooth Disk with Inlet Hub Inlet Dia/Hub Dia = 1.33
II	13	water	0.080	0	0	Smooth Disk with Inlet Hub Inlet Dia/Hub Dia = 2.00
II	14	water	0.065	0.125	24	Bladed Disk with Tip Blockage, Tip Clearance = 0.100
II	15	water	0.065	0.125	24	Bladed Disk with Tip Blockage, Tip Clearance = 0.050
II	16	water	0.065	0.125	24	Bladed Disk with Tip Blockage, Tip Clearance = 0.150
II	17	water	0.065	0.125	24	Bladed Disk
II	18	water	0.138	0	0	Smooth Disk

Table III-1. Summary of Tests (Continued)

Test Phase	Test No.	Test Fluid	Axial Clearance, in.	Blade Height, in.	Number of Blades	Remarks
II	19	LH ₂	0.138	0	0	Smooth Disk
II	20	LH ₂	0.065	0	0	Smooth Disk
II	21	LH ₂	0.024	0	0	Smooth Disk
II	22	LH ₂	0.065	0	0	Smooth Disk with Inlet Hub Inlet Dia/Hub Dia = 2.00
II	23	LH ₂	0.140	0.250	24	Bladed Disk
II	24	LH ₂	0.065	0.250	24	Rig Failure Terminated Test
II	25	LH ₂	0.035	0.125	24	Bladed Disk
II	26	LH ₂	0.073	0.125	24	Bladed Disk
II	27	LH ₂	0.073	0.125	24	Bladed Disk with Tip Blockage Tip Clearance = 0.050
II	28	LH ₂	0.073	0.125	24	Bladed Disk with Tip Blockage Tip Clearance = 0.150
II	29	LH ₂	F=0.156 R=0.135	0.125	24	Bladed Disk F = Front R = Rear
II	30	LH ₂	0.073	0.125	24	Bladed Disk with Tip Blockage Tip Clearance = 0.100
II	31	LH ₂	0.074	0.125	12	Bladed Disk
II	32	LH ₂	0.075	0.125	6	Bladed Disk
II	33	LH ₂	0.072	0.250	24	Bladed Disk
II	34	LH ₂	0.037	0.250	24	Bladed Disk

Table III-1. Summary of Tests (Continued)

Test Phase	Test No.	Test Fluid	Axial Clearance, in.	Blade Height, in.	Number of Blades	Remarks
II	35	LH ₂	0.057	0	0	Smooth Disk
II	36	LH ₂	0.057	0	0	Smooth Disk with Inlet Hub Inlet Dia/Hub Dia = 2.00
II	37	LH ₂	0.057	0	0	Smooth Disk Reversed Flow
II	38	water	0.057	0	0	Smooth Disk with Inlet Hub Inlet Dia/Hub Dia = 2.00
III	39	water	0.057	0	0	Smooth Disk
III	40	LH ₂	0.055	0	0	Smooth Disk High Pressure Test Inlet Pressure = 650 psia
III	41	LH ₂	0.032	0.125	24	Bladed Disk with Tip Blockage Tip Clearance = 0.100
III	42	LH ₂	0.055	0.125	24	Bladed Disk with Tip Blockage Tip Clearance = 0.100
III	43	LH ₂	0.055	0.125	24	Bladed Disk with Tip Blockage Tip Clearance = 0.050
III	44	LH ₂	0.039	F=0.139 R=0.131	24	Bladed housings Smooth Disk Blade Heights: F = Front R = Rear
III	45	LH ₂	F=0.128 R=0.038	F=0.139 R=0.131	24	Bladed Housings Smooth Disk Unequal Clearances: F = Front R = Rear

Table III-1. Summary of Tests (Continued)

Test Phase	Test No.	Test Fluid	Axial Clearance, in.	Blade Height, in.	Number of Blades	Remarks
III	46	water	F=0.128 R=0.038	F=0.139 R=0.131	24	Bladed Housings Smooth Disk
III	47	water	F=0.082 R=0.038	F=0.139 R=0.131	24	Bladed Housing Smooth Disk

Several special cases of the variation of β with radius have been categorized. A forced vortex is common to the pumping face of a centrifugal pump and occurs if the angular velocity is constant with radius, which results in a straight-line pressure-radius squared curve, as shown in figure III-1. A free vortex is common to inward flow on a rotating smooth disk and occurs when the angular velocity varies inversely with the disk radius squared. The free vortex case yields a nonlinear pressure-radius squared curve with the slope decreasing with increasing radius as shown in figure III-2.

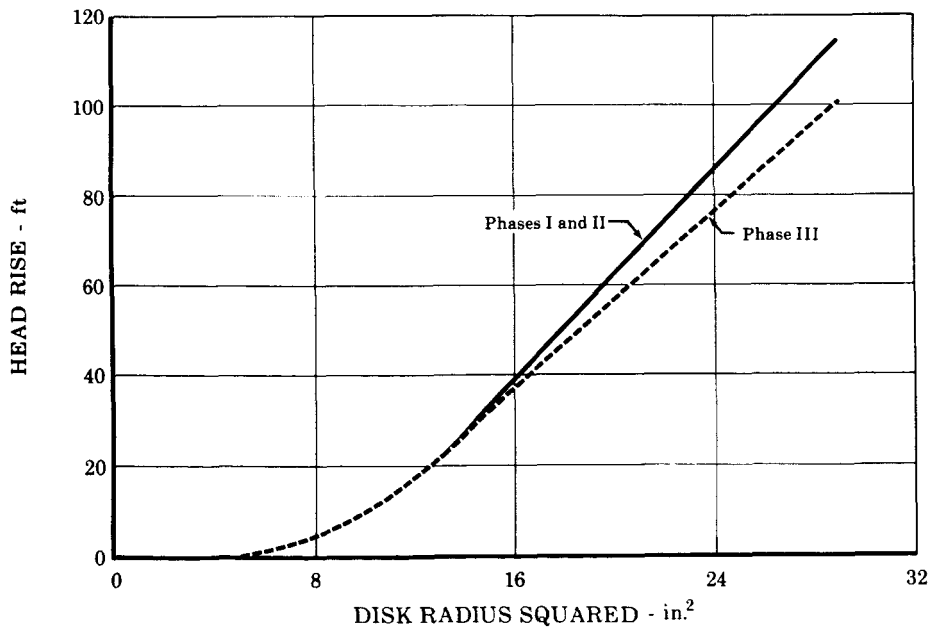


Figure III-1. Radial Head Distribution for Smooth Disk in Water, Radially Outward Flow FD 7814A

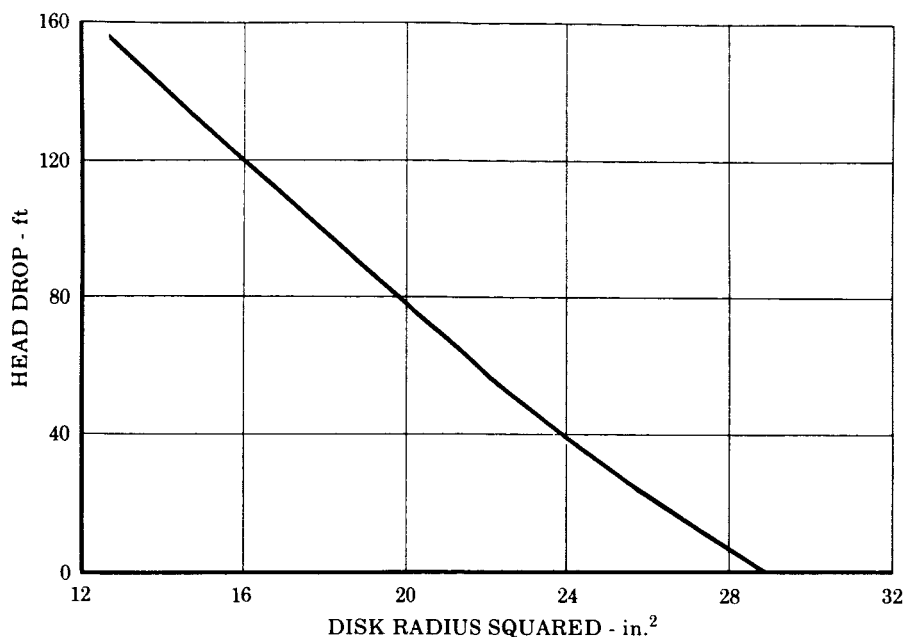


Figure III-2. Radial Head Distribution for Smooth Disk in Water, Radially Inward Flow

The vortex mode that actually exists in a pump depends on various factors mentioned previously, and the analytical prediction of the vortex mode for a particular application so as to arrive at accurate values of angular velocity and in turn the corresponding pressure distribution would be very complex. Therefore, the following approach was used to provide an empirical solution for equation (III-1).

$$\int dP = \int \frac{\gamma}{g} \beta^2 R dR \quad (\text{III-1})$$

1. The fluid velocity, β , can be replaced by a fraction, K , of the disk rotational speed:

$$\beta = K\omega \quad (\text{III-2})$$

2. Equation (III-1) is integrated within the radius limits of the disk, R_1 to R_2

$$\frac{P_2 - P_1}{\gamma} = \frac{K^2 \omega^2}{2g} (R_2^2 - R_1^2) \quad (\text{III-3})$$

or in the case where γ is not constant from 1 to 2

$$\frac{P_2}{\gamma_2} - \frac{P_1}{\gamma_1} = \frac{K^2 \omega^2}{2g} (R_2^2 - R_1^2) \quad (\text{III-4})$$

where

$$\frac{P_2}{\gamma_2} = H_2 \text{ and } \frac{P_1}{\gamma_1} = H_1$$

3. Because the fraction K was considered a constant in the integration, it can be made a function of any variable that is thought to influence the fluid angular velocity, β , such as

$$K = f(R, C, T, N_B, Re, \text{ etc.})$$

and determined experimentally.

4. When K is found to be a function of radius, R , the head distribution becomes:

$$\sum_{i=1}^n (H_{i+1} - H_i) = \sum_{i=1}^n \frac{K_i^2 \omega^2}{2g} (R_{i+1}^2 - R_i^2) \quad (\text{III-5})$$

and the head rise is summed over the disk radius.

In the following paragraphs a discussion of the experimentally determined head rise values is presented.

C. DISCUSSION OF TEST RESULTS

1. Smooth Disk, Smooth Housing - Water

For the smooth disk in a smooth housing with outward flow, the Phases I and II data resulted in a straight line ΔH vs R^2 plot as shown in figure III-1, except for a small area at the disk center. The straight line shows that a forced vortex exists over most of the radial span. The Phase III smooth disk data verified this straight line distribution, but the slope of the curve was less than those from Phases I and II as also shown in figure III-1. This deviation is attributed to slots in the housing wall that probably created local flow disturbances along the flow path resulting in a reduced fluid velocity and, therefore, a reduced head rise. These slots were required for the special Rosemount temperature probes used in the Phase III liquid hydrogen tests to determine the temperature profile.

For the smooth disk with inward flow, the data resulted in a ΔH vs R^2 curve that was not a straight line, (see figure III-2). The shape of the curve indicates that the vortex mode is changing with radius. In addition it was found that the slope of the ΔH vs R^2 curve was affected by clearance and flow coefficient for both inward and outward flow.

A portion of the studies in Phases II and III was devoted to determining the effect of the addition of an inlet hub on the smooth disk head distribution. (See the insert in figure II-1.) The Phase II study included two hub sizes, with inlet diameter to hub diameter ratios of 1.33 and 2.00. There was no appreciable difference in the results obtained between the two hubs tested (see figure III-3). By comparing the ΔH vs R^2 curves from Phase II it was determined that the addition of an inlet hub, while causing a more rapid acceleration of the fluid at the inlet, decreased the slope of the curve resulting in a lower overall head rise. However, the data from Phase III showed no effect on head rise by the addition of an inlet hub. It appears from the results of these tests that the decrease in the slope of the ΔH vs R^2 curves, caused by the addition of a hub in the Phase II tests, may be attributed to increased turbulence. In the Phase III testing the head rise on the smooth disk without a hub was probably decreased because of the turbulence caused by the slots in the housing, as mentioned previously, thereby masking the effect of adding the inlet hub. This theory is supported in part by the fact that the head rise in the Phase II hub test was nearly identical to the head rise of the hubless test in Phase III.

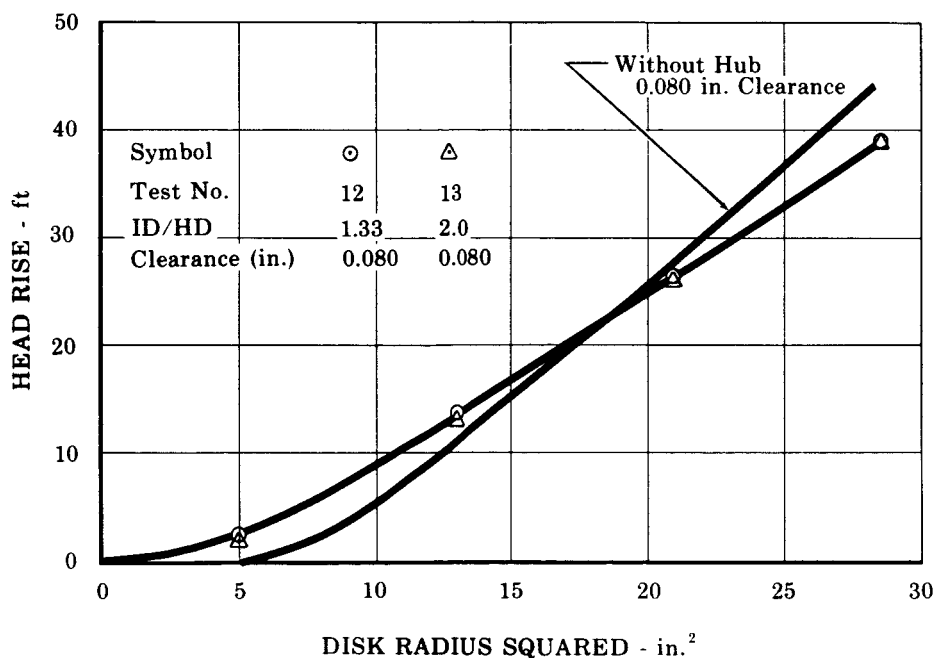


Figure III-3. Radial Head Distribution for Smooth Disk with Inlet Hub in Water, Radially Outward Flow FD 10999A

2. Smooth Disk, Smooth Housing - Hydrogen

The smooth disk and smooth housing configuration was tested in liquid hydrogen in Phases II and III. A typical ΔH vs R^2 plot for a test with outward flow is shown in figure III-4. As this curve shows, the head distribution describes a straight line as was the case in water. For inward flow (figure III-5) the ΔH vs R^2 curve is similar in shape to the inward flow smooth disk case in water with the vortex mode being dependent on radius ratio, clearance, and flow coefficient.

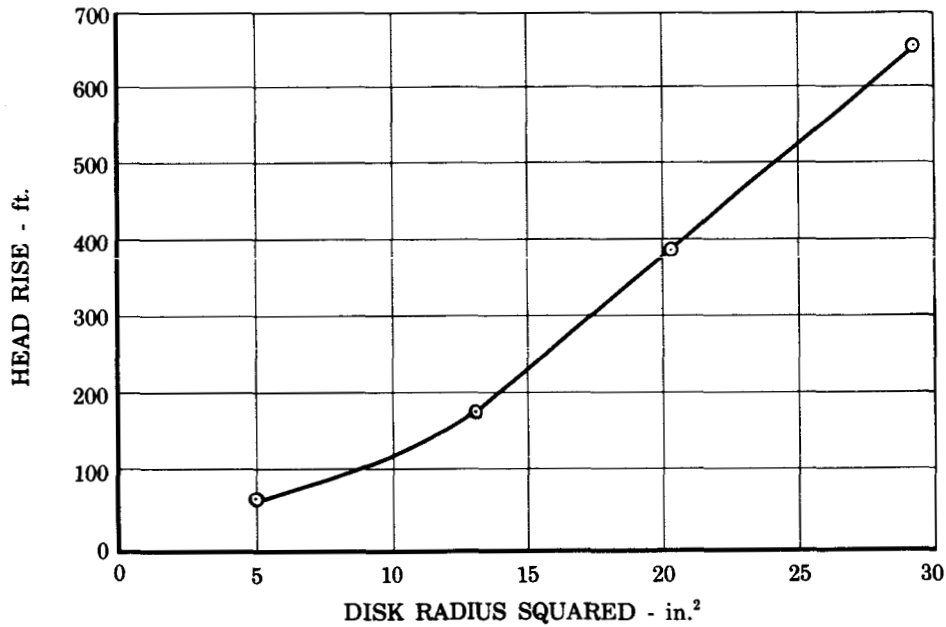


Figure III-4. Radial Head Distribution for Smooth FD 14555A Disk in Liquid Hydrogen, Radially Outward Flow

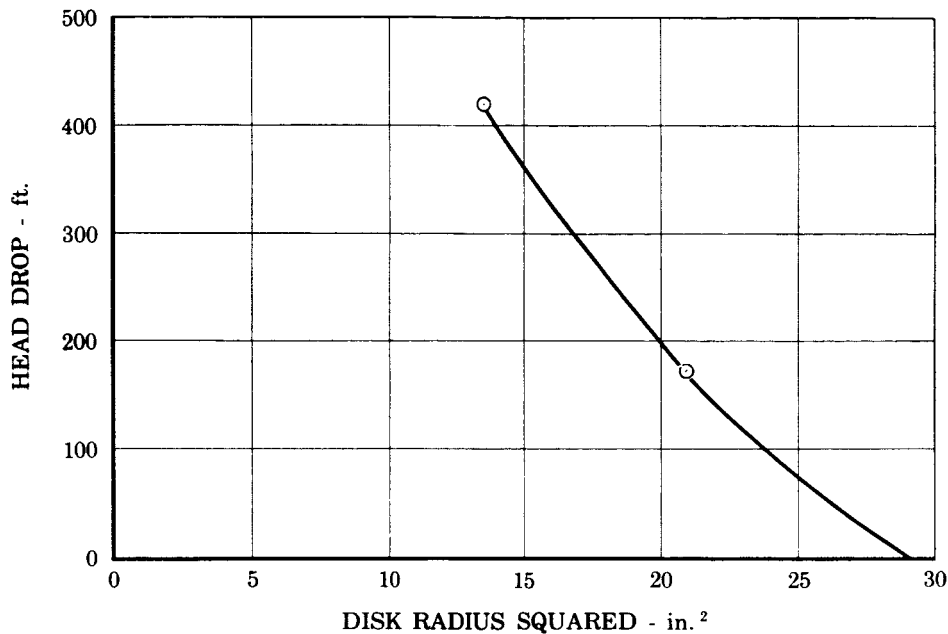


Figure III-5. Radial Head Distribution for Smooth Disk in Liquid Hydrogen, Radially Inward Flow FD 14554

The addition of an inlet hub to the smooth disk in liquid hydrogen tended to increase the overall head rise for the outward flow case in Phase II. This was in opposition to the Phase II water tests where the overall head rise decreased with the addition of the inlet hub. There is at present no complete explanation for the difference in results between the two fluids; however, one possibility is that the lower viscosity and density of the hydrogen may reduce the amount of turbulence, and thus the initial acceleration imparted to the fluid by the hub would not be destroyed and the fluid velocity along the disk would be proportionally higher.

The Phase III liquid hydrogen test results, like the Phase III water tests, showed lower fluid velocities than in Phase II. Also, the addition of an inlet hub had less effect than was noted in the Phase II testing. This discrepancy between the Phase II and III results is attributed to the special Rosemount temperature probes. The losses created by the slots that accommodated the probes could also reduce the effect of the inlet hub.

The smooth disk inward flow data were extended to lower radius values in Phase III by reverse flowing the test apparatus with liquid hydrogen. Under conditions of reverse flow, inward flow would be achieved on the front side of the rotating disk providing pressure instrumentation at radius squared values of 29, 21, 13, and 5 in.², whereas with normal flow direction, pressure data were obtainable only at radius squared values of 29, 21, and 13 in.². The results of the tests were affected by a severe pressure drop at the inlet (normally the discharge) which caused cavitation or boiling within the flow passage. Therefore, usable data were limited to very low flow coefficients. These data were generally in good agreement with data from previous tests and were used to modify the smooth disk, inward flow regression equation for K.

3. Bladed Disk, Smooth Housing

The Phase I study, with water as the test fluid, produced consistent results for both 0.125- and 0.250-inch high blades with 24-bladed disks. Typical ΔH vs R^2 curves for outward and inward flow conditions (figures III-6 and III-7) show that the data lie on a curved line, and therefore the fluid angular velocity is not constant over the disk radial span. The Phase I data also showed that flowrate had no effect on the ΔH vs R^2 curves.

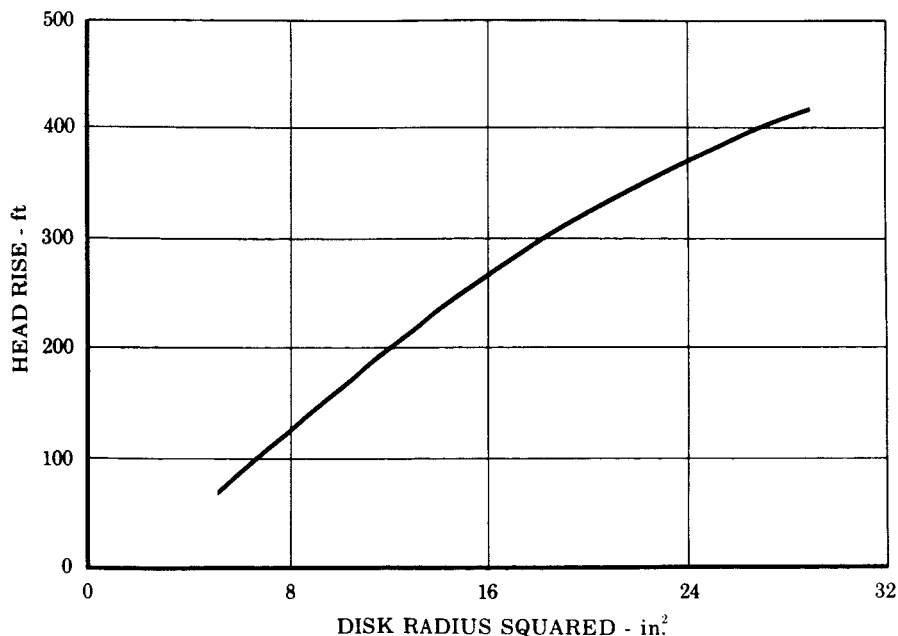


Figure III-6. Radial Head Distribution for Bladed Disk in Water, Radially Outward Flow FD 7840A

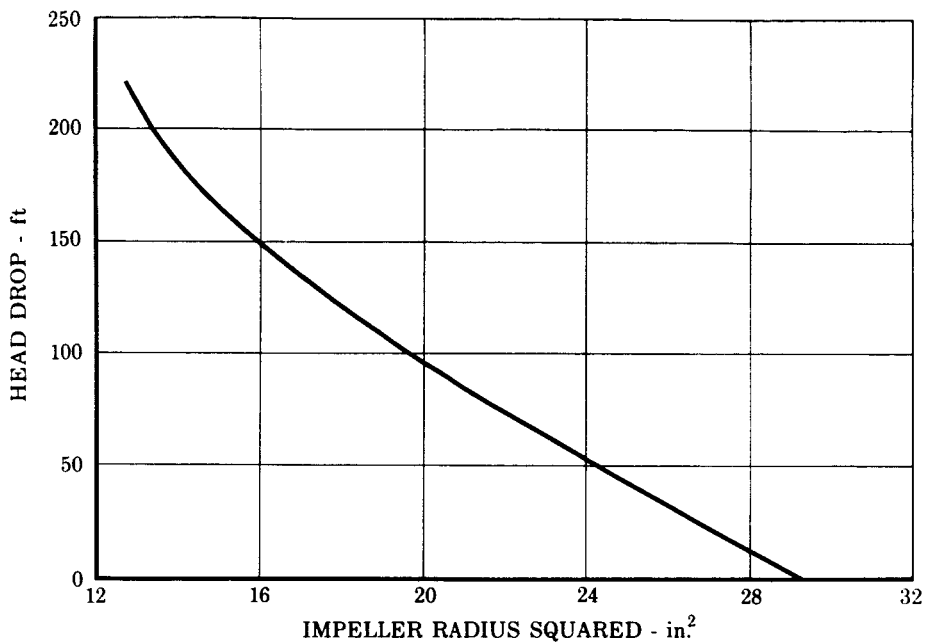


Figure III-7. Radial Head Distribution for Bladed Disk in Water, Radially Inward Flow FD 7821A

The effect on head distribution of reducing the number of blades was also studied under Phase I. A 0.125-inch blade height disk was tested with 12 and 6 blades at constant clearance. The test results show a relatively small effect of blade number on the head distribution for inward and outward flow.

These same disk configurations were tested in Phase II with liquid hydrogen as the test fluid. Typical ΔH vs R^2 curves are shown in figure III-8. The head distribution plotted as a straight line for all values of clearance, blade height, and blade number for outward flow. The inward flow case yielded a head distribution similar to all previous cases: that is, a curved ΔH vs R^2 line.

The effect of disk tip blockage was investigated in both water and liquid hydrogen in Phases II and III. The tip blockage simulates the condition of a housing overhang at the impeller tip. For outward flow with water, the ΔH vs R^2 plot tends toward a straight line as shown in figure III-9, but overall head rise is not affected. There was negligible effect on the head distribution for inward flow as also shown in figure III-9.

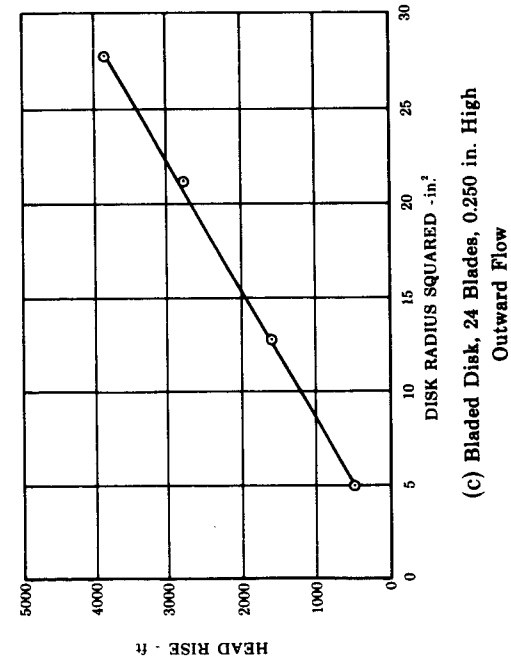
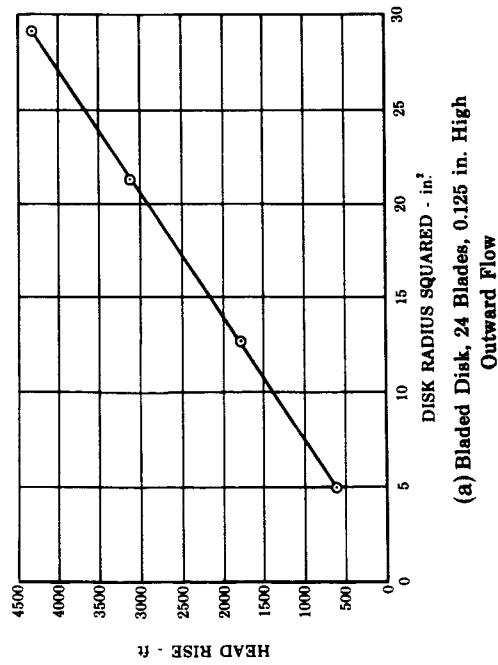
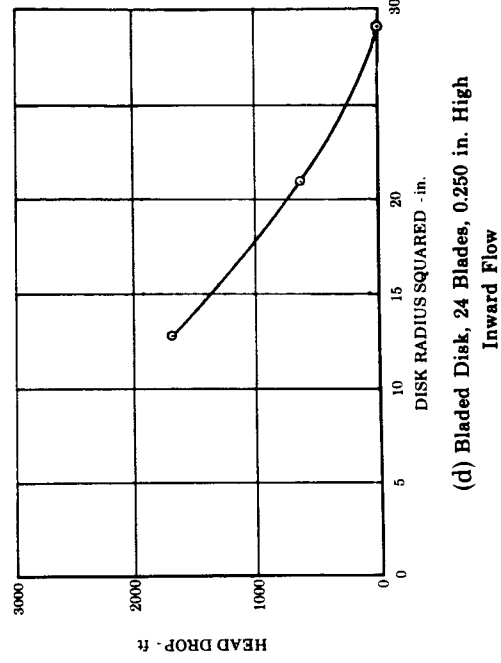
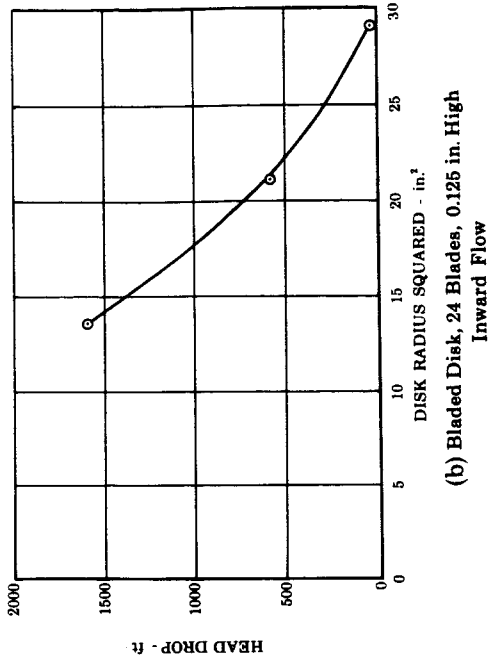
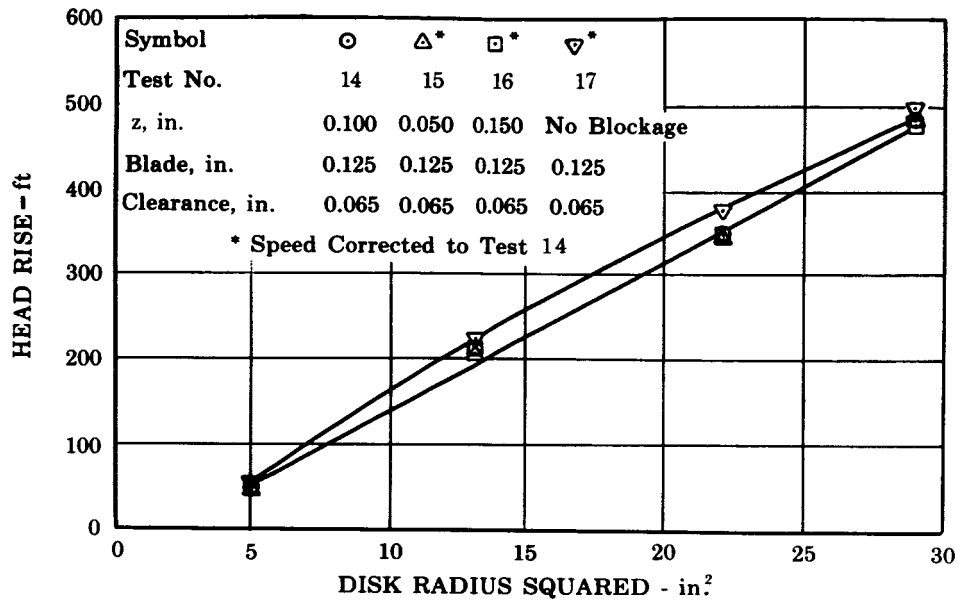
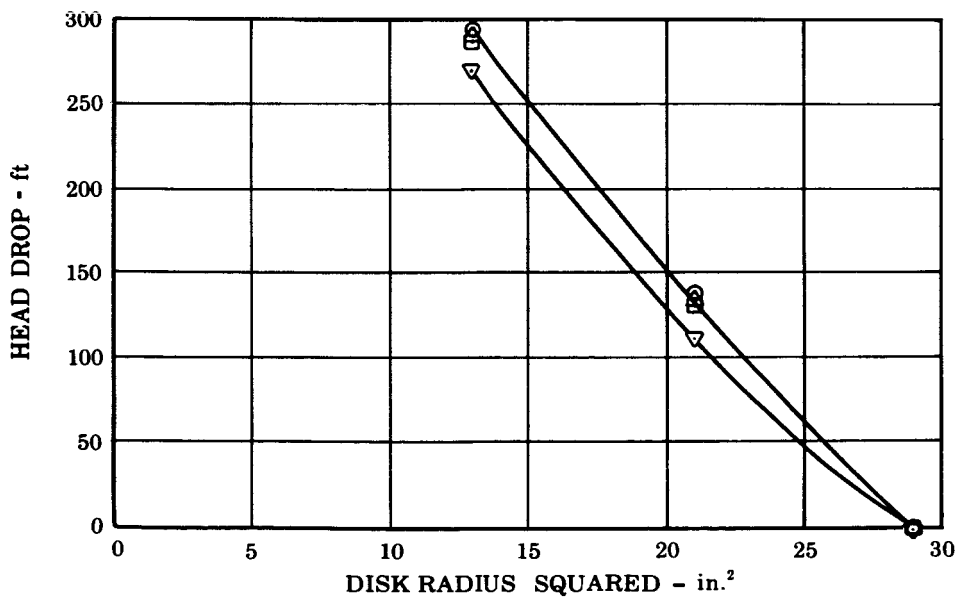


Figure III-8. Typical Radial Head Distribution for Bladed Disks in Liquid Hydrogen



(a) Radially Outward Flow



(b) Radially Inward Flow

Figure III-9. Radial Head Distribution for Bladed Disk with Tip Blockage in Water

FD 10998A

For liquid hydrogen, the results showed that the addition of tip blockage had no measurable effect on head distribution for both the inward and outward flow. The only change noted by the addition of tip blockage was a significant increase in liquid hydrogen temperature at the disk discharge annulus over the tests without tip blockage. This increase in temperature was first noted in the Phase II testing and was believed to be caused by fluid friction in the annulus between the tip of the disk and the blockage rings. The special Rosemount surface temperature probes were installed in Phase III and verified this theory. The temperature rise along the face of the disk was the same with or without tip blockage and there was an increase in temperature across the annulus between the disk and the blockage ring. The fluid friction on this annulus was also reflected by an increase in torque required to drive the rotor but the exact increase could not be determined because of scatter in the test data.

4. Smooth Disk, Bladed Housing

The four tests conducted on this configuration included two in liquid hydrogen and two in water with different blade-to-disk axial clearances. The results show that no measurable head rise was generated with outward flow and no head drop with inward flow, indicating essentially no fluid rotation.

5. Torque Measurements

Data on the energy input to the rotating disk were obtained by means of the torque measuring device described in Section II. Consistent data were obtained in the water tests but, because of the low power requirements in liquid hydrogen and difficulties encountered with the torque measuring device, the data from the hydrogen tests were erratic and are considered invalid.

Figure III-10 shows the torque data from a smooth disk, smooth housing test in water plotted as torque coefficient, C_m , versus disk Reynolds number, Re , at the tip of the disk. There was fairly close agreement between these data and that of Daily and Nece (Reference 1) and with the theoretical equations of Schultz-Grunow (Reference 2). Clearance and flow coefficient had no measurable effect on the torque coefficient within the range tested.

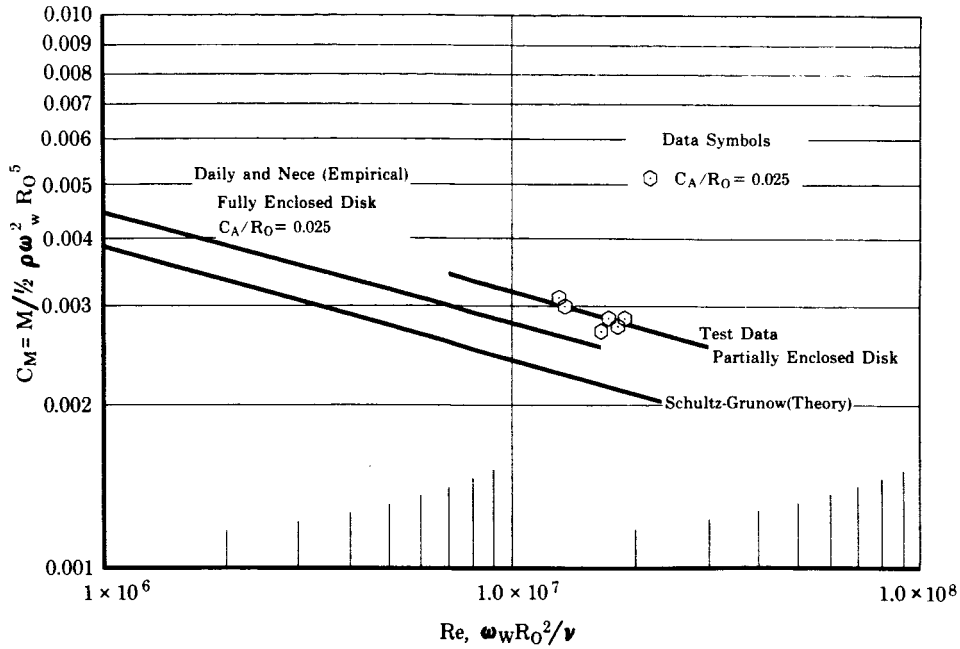


Figure III-10. Smooth Disk Torque Data

FD 7837A

Plots of torque coefficient versus Reynolds number for the bladed disk in water are shown in figure III-11. These curves show the effect of blade height, T, and the ratio of blade height to the sum of blade height plus clearance, T/S, and reflect the increase in power required for greater blade heights and/or increased clearance.

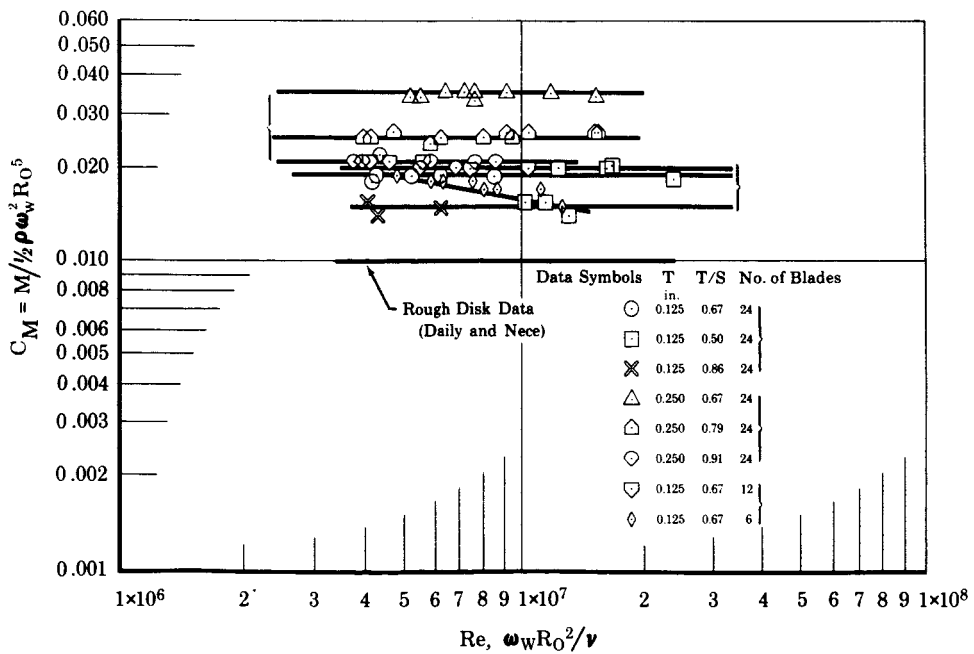


Figure III-11. Bladed Disk Torque Data

FD 7838B

The torque measurements included the rim drag of the disk, so a calculation of disk rim friction was necessary for a valid comparison of data. The method of Daily and Nece (Reference 1) for turbulent flow was used in this calculation. The method considers the annulus between the disk and the wall as a duct analogous to a circular pipe. The shear stress on the disk rim was given as,

$$\tau = (f/4)(p/2)(\omega R_o/2)^2$$

This expression is used in deriving the correction for C_M expressed as,

$$C'_M = \frac{f \pi b}{8 R_o}$$

and, hence,

$$C_M \text{ actual} = C_M \text{ measured} - C'_M$$

The friction factor, f , was determined from the smooth pipe curve on a Moody diagram using a Reynolds number given as,

$$Re = \frac{\omega R_o C}{\nu}$$

where:

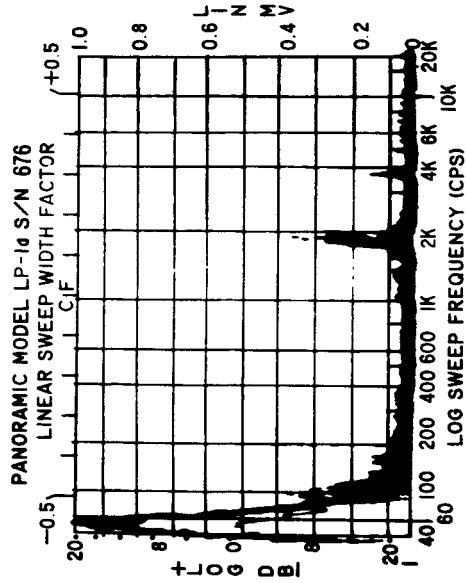
$$C = \text{Disk tip clearance}$$

Daily and Nece found by experimenting with smooth disks of various thickness that this correction method was valid. Values of C'_M for the testing performed in this report ranged from 0.0010 to 0.00133.

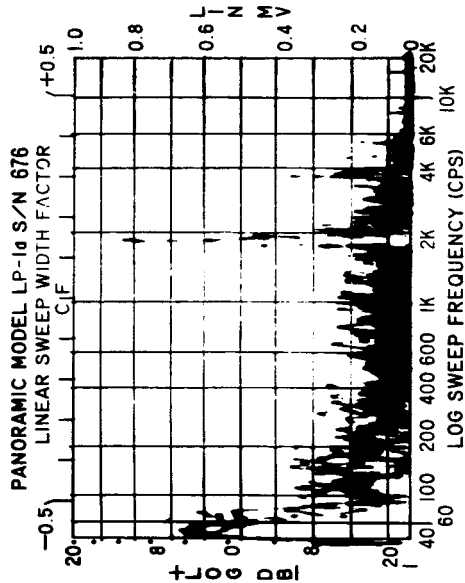
6. Blade-to-Blade Pressure Oscillations

The pressure pulses generated by a blade sweeping past a high response pressure transducer (refer to Section II) were recorded on magnetic tape during the bladed disk tests. These tapes were analyzed on a multi-channel wave analyzer, and photographs taken of typical test points are shown in figures III-12 and III-13 for water and liquid hydrogen, respectively. Each photograph is a display of the peak-to-peak pressure amplitudes at the frequency of the complex wave generated by the passing blade. Several pressure pulses appear on each illustration. The pulse of primary interest in this study occurs at the frequency of the passing blade. At higher frequencies harmonics appear. With the 24-blade rotor the amplitudes of the harmonics were quite low; however, for the 12- and 6-blade disk the higher harmonics were quite distinct. At the disk,

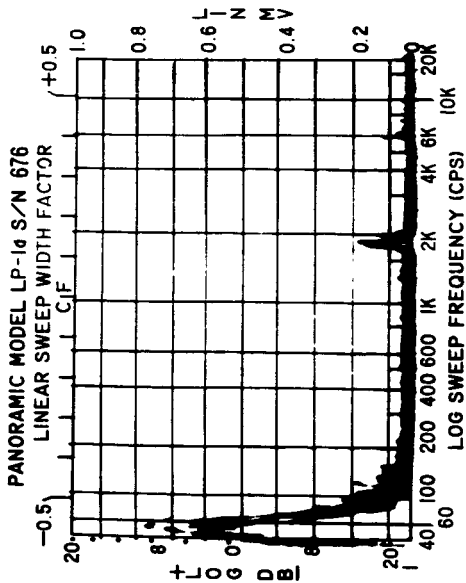
rotating frequency pulses were also visible and were probably caused by a slight axial runout of the disk. A blade pressure loading parameter was calculated from the data and plotted against radius ratio squared as shown in figures III-14 and III-15 for water and liquid hydrogen, respectively. The blade pressure loading parameter was defined as the peak-to-peak pressure pulse at the blade passing frequency divided by the local average static pressure (or $\Delta p/P$). The $\Delta p/P$ data for the water tests were scattered but can be approximated by a constant value of 0.075 independent of speed, clearance, radius ratio, and number of blades. There did not appear to be a readily predictable trend from the data plotted for liquid hydrogen.



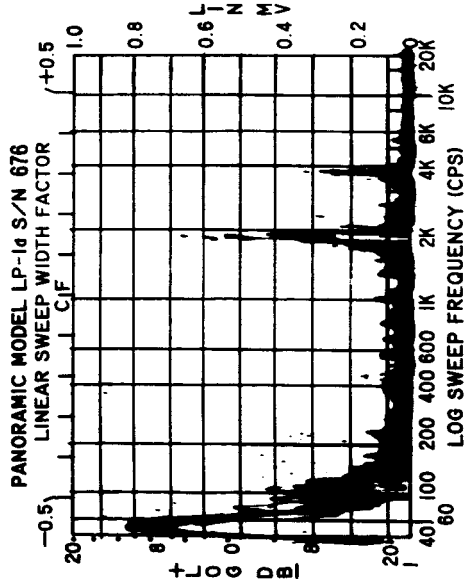
$R/R_0 = 0.66$



$R/R_0 = 1.00$

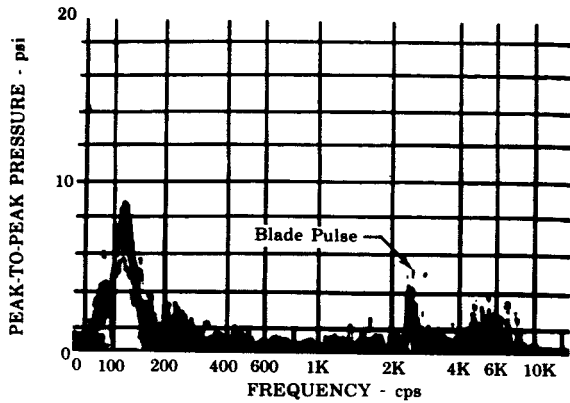


$R/R_0 = 0.85$

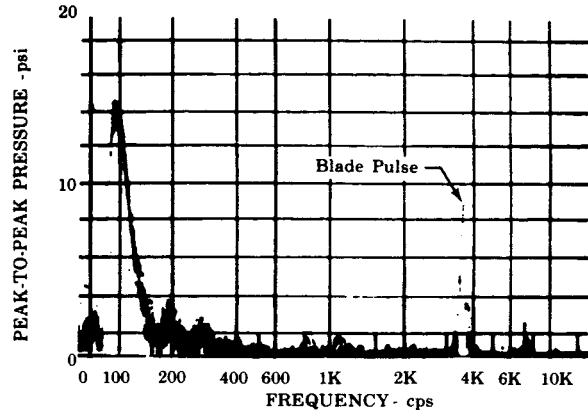


$R/R_0 = 0.66$

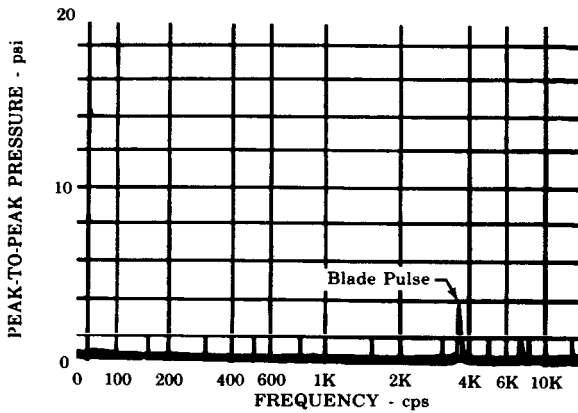
Figure III-12. Typical Panoram Wave Analysis of Bladed Disk Test in Water



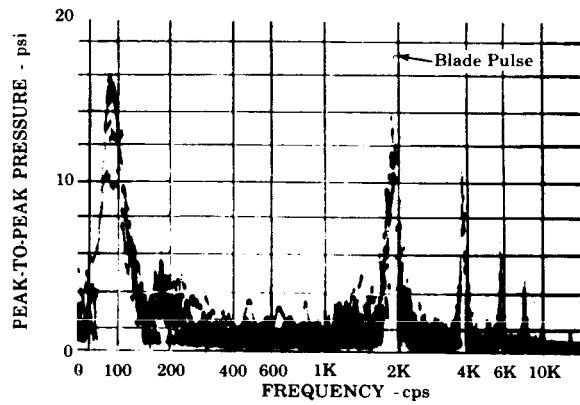
(a) Test 23 24 Blades
 $T = 0.250$ in. $C = 0.140$ in.



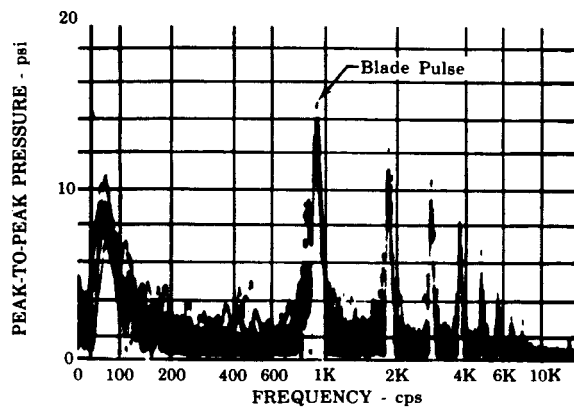
(b) Test 26 24 Blades
 $T = 0.125$ in. $C = 0.073$ in.



(c) Test 27 24 Blades
 $T = 0.125$ $C = 0.073$ in.
 $z = 0.050$ in.



(d) Test 31 12 Blades
 $T = 0.125$ in. $C = 0.074$ in.



(e) Test 32 6 Blades
 $T = 0.125$ in. $C = 0.075$ in.

Figure III-13. Typical Peak-to-Peak Pressure vs Frequency

FD 11002A

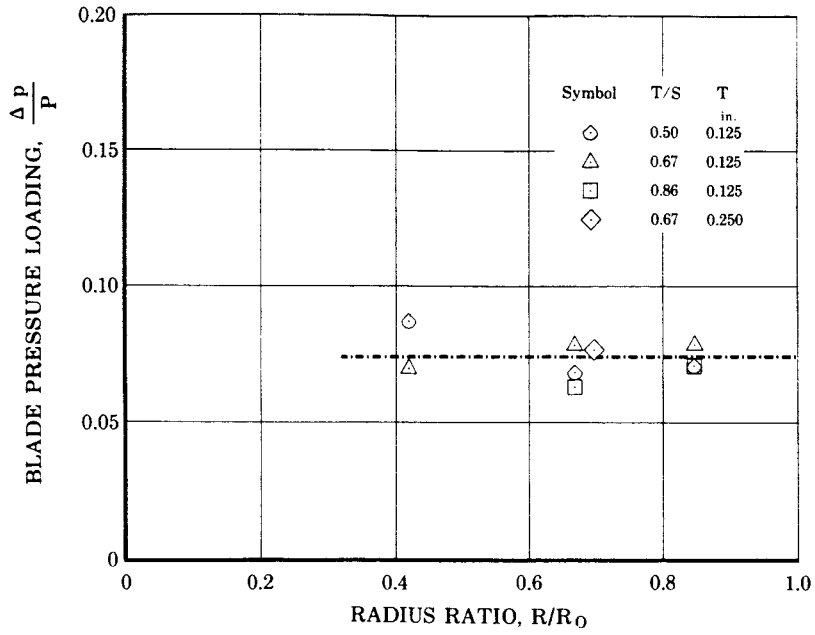
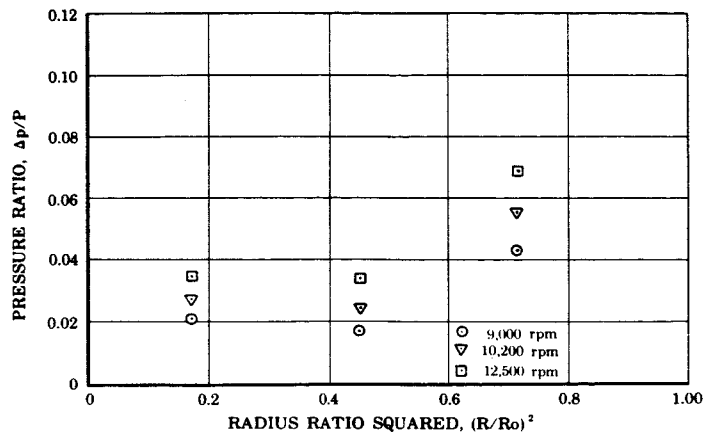
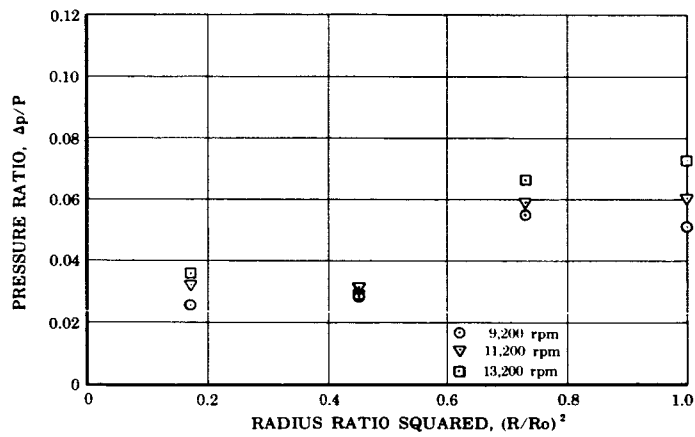


Figure III-14. Blade Pressure Loading

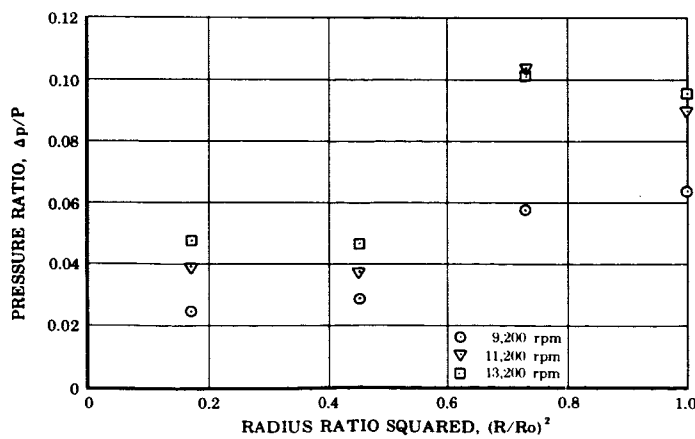
FD 7812A



(a) 24 Blades $T = 0.125$ in.,
 $C = 0.035$ in.



(b) 24 Blades $T = 0.125$ in.,
 $C = 0.074$ in.



(c) 24 Blades $T = 0.125$ in.,
 $C = 0.156$

Figure III-15. Blade Pressure Loading vs Radius Ratio Squared for Bladed Disk in Liquid Hydrogen FD 11001A

SECTION IV
DETERMINATION OF K VALUES

As mentioned previously in Section III, the vortex mode for any case of rotating flow may be determined by evaluating K as a function of the influencing variables. K was calculated for each configuration and flow condition investigated from the slopes of the ΔH vs R^2 curves. The equation for K is as follows:

$$K = \sqrt{\frac{2g(H_2 - H_1)}{\omega^2(R_2^2 - R_1^2)}} \quad (IV-1)$$

For the case where the ΔH vs R^2 curve was not linear (i.e., not a forced vortex) the K value was determined as a function of radius by dividing the $\Delta H - R^2$ curve into a number of small straight-line segments (each approximating a forced vortex) and calculating a K for each segment. The radius ratio for each segment was obtained by dividing the radius at the midpoint of the segment by the outer radius of the disk.

Generally, for radially outward flow, K was determined to be a function of flow coefficient and clearance for the smooth disk in both hydrogen and water. For the bladed disk in water, K was determined to also be a function of clearance ratio, radius ratio, and blade height. For the bladed disk in liquid hydrogen, K was determined to be constant and equal to unity for all cases. The bladed-housing smooth-disk test did not yield any change in head, so that the K value was essentially zero for all flow conditions tested.

The head distribution data were used to derive the following regression equations for K as a function of the significant variables by the methods previously described. The maximum percent error (MPE) and the average percent error (APE) in the fit of the data to the equations is given with each equation.

1. Smooth Disk, Smooth Housing

For Water - Outward Flow

$$K = 0.578 - 4.11\phi - 1.67C \quad (IV-2)$$

$$MPE = 4.5\% \quad APE = 2.0\%$$

For Water - Inward Flow

$$\begin{aligned}
 K &= 0.3865 + 95.3 \phi^2 - 12.6 \phi \left(\frac{R}{R_o}\right)^2 - 9.17 \times 10^5 \phi \left(\frac{C}{R_o}\right)^3 \quad (\text{IV-3}) \\
 &+ 27.8 \left(\frac{R}{R_o}\right)^2 \left(\frac{C}{R_o}\right) - 2.75 \times 10^3 \left(\frac{R}{R_o}\right)^4 \left(\frac{C}{R_o}\right)^2 + 6.51 \times 10^4 \left(\frac{R}{R_o}\right)^6 \left(\frac{C}{R_o}\right)^2 \\
 &+ 2.13 \phi^{0.5} - 6.59 \left(\frac{C}{R_o}\right)
 \end{aligned}$$

$$\text{MPE} = 28.6\%$$

$$\text{APE} = 4.92\%$$

For LH₂ - Outward Flow

$$K = 0.906 + 0.012 \phi \left(\frac{C}{R_o}\right)^{-1.0} - 5.36 \phi - 51.1 \left(\frac{C}{R_o}\right) + 1295.3 \left(\frac{C}{R_o}\right)^{2.0} \quad (\text{IV-4})$$

$$\text{MPE} = 29.2\%$$

$$\text{APE} = 5.54\%$$

For LH₂ - Inward Flow

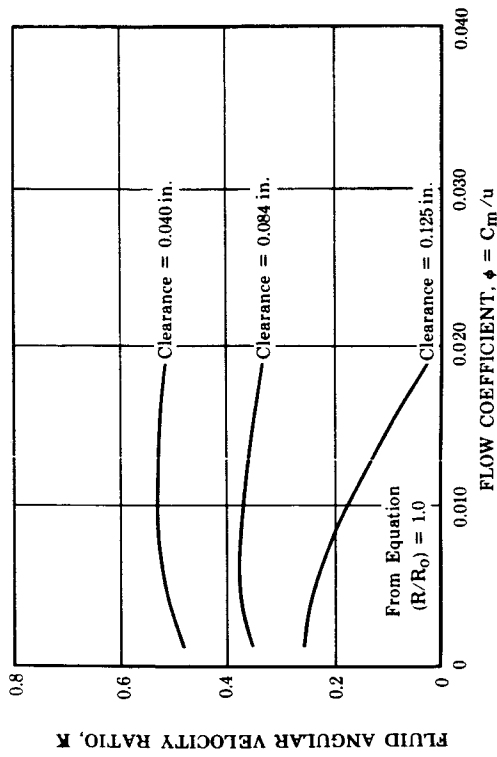
$$K = 0.18 \phi^{0.016} \left(\frac{R}{R_o}\right)^{-1.434} C^{-0.233} \quad (\text{IV-5})$$

$$\text{MPE} = 4.12\%$$

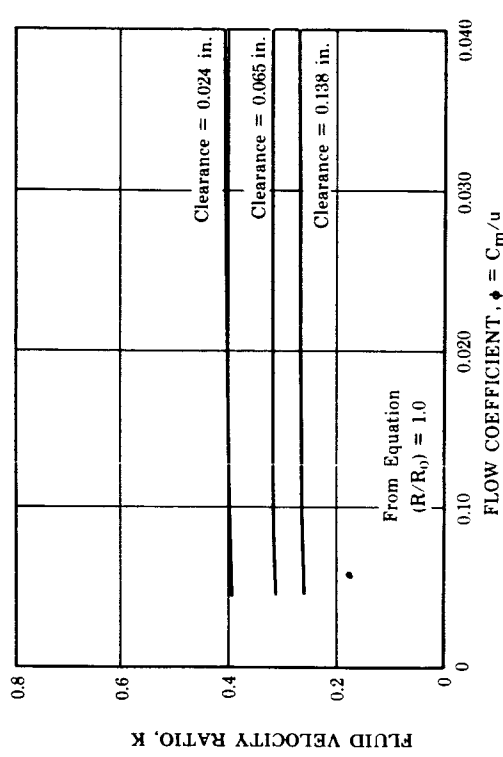
$$\text{APE} = 1.69\%$$

Figure IV-1 shows plots of K vs flow coefficient for the smooth disk in water with radially outward and inward flow. For outward flow, K is a function of clearance (C) and flow coefficient (ϕ) but independent of radius. For inward flow K is a function of radius as well as the other two. Figure IV-1 also shows the same plots for liquid hydrogen. As in the case of water, K is a function of C and ϕ for outward flow and C, ϕ and R for inward; however, the effect of flow coefficient with inward flow is slight and can be considered negligible between $\phi = 0.010$ and 0.040.

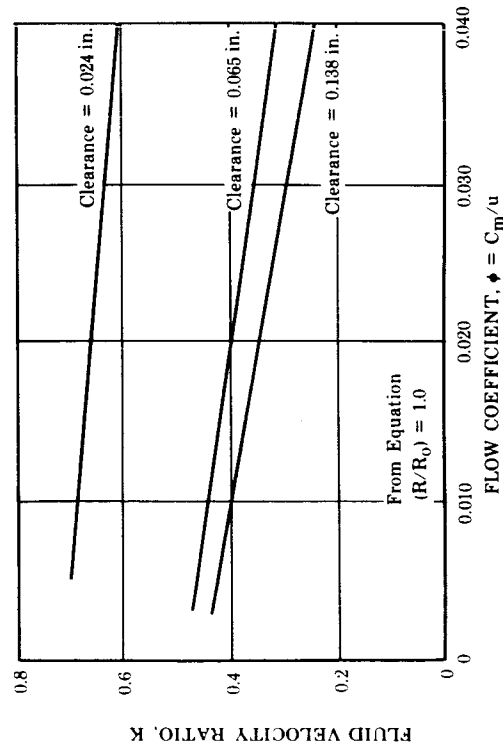
Figure IV-2 shows cross-plots of the same variables showing the change in K with clearance. Of particular interest is the difference between the two fluids for the outward flow case; K is a linear function of clearance in water and nonlinear in hydrogen.



(b) Water Inward Flow



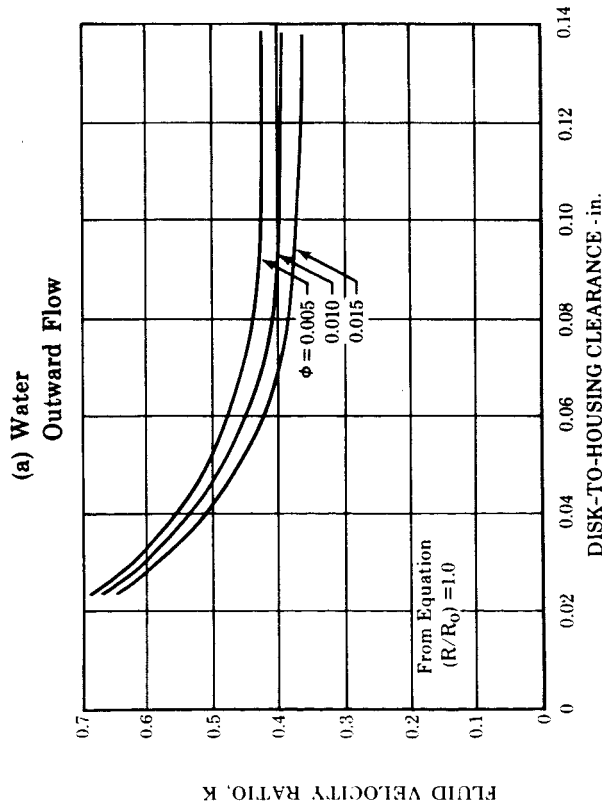
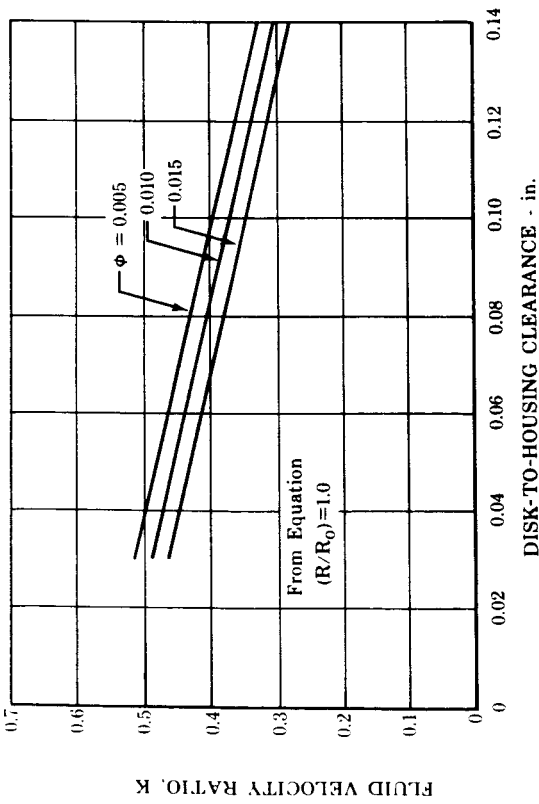
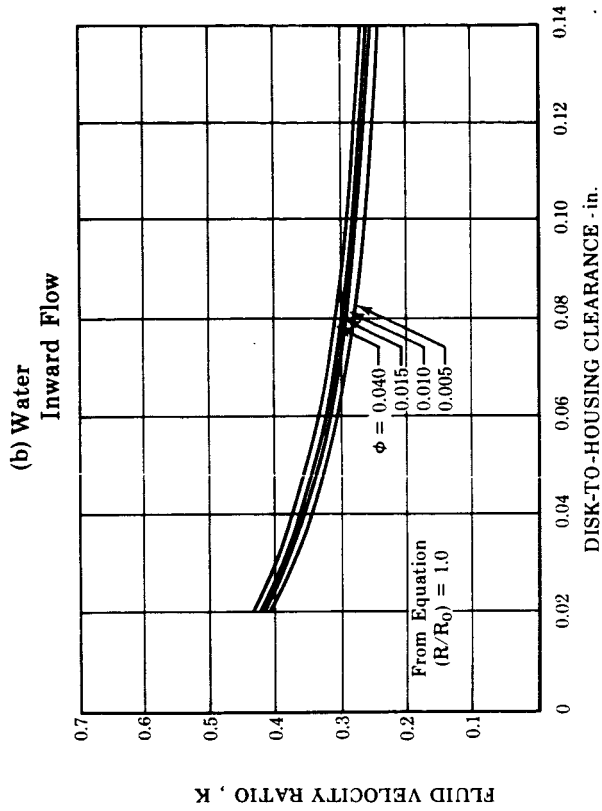
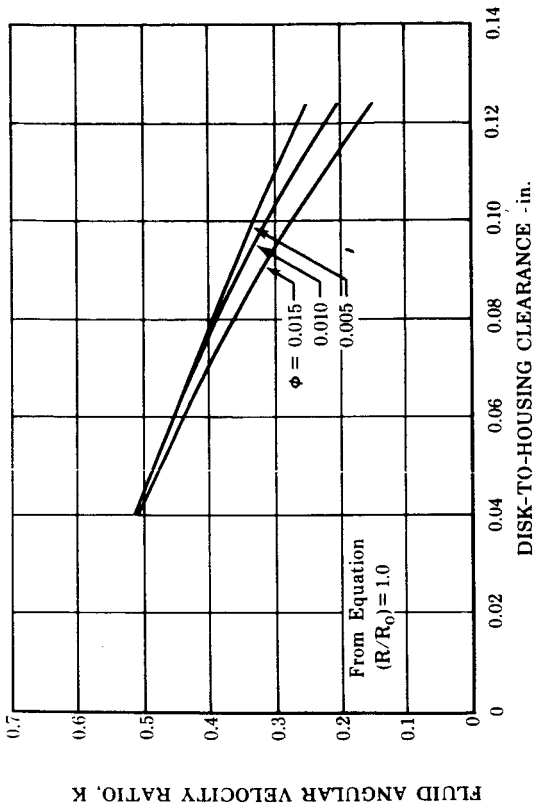
(c) LH₂ Outward Flow



(d) LH₂ Inward Flow

Figure IV-1. Fluid Velocity Ratio vs Flow Coefficient for Smooth Disk

FD 10987B



FD 10982A

Figure IV-2. Fluid Velocity Ratio vs Disk-to-Housing Clearance for Smooth Disk

2. Bladed Disk, Smooth Housing

For Water - Inward and Outward Flow

$$K = 0.951 - 0.282 \left(\frac{R}{R_o} \right) + 0.2137 \left(\frac{T}{S} \right) + 0.175 T \quad (IV-6)$$

$$MPE = 6.0\%$$

$$APE = 2.5\%$$

For LH₂ - Outward Flow

$$K = 1.0 \text{ (Both blade heights)}$$

$$MPE = 5.0\%$$

$$APE = 1.69\%$$

For LH₂ - Inward Flow

(a) Blade Height = 0.250 inch

$$K = -0.8819 + 1.24 \left(\frac{R}{R_o} \right)^2 - 1.94 \left(\frac{R}{R_o} \right)^4 + 0.841 \left(\frac{R}{R_o} \right)^6 \quad (IV-7)$$

$$+ 4.06 \left(\frac{T}{S} \right) - 2.41 \left(\frac{T}{S} \right)^2 - 23.9 \left(\frac{R}{R_o} \right)^2 \phi + 1283.1 \left(\frac{R}{R_o} \right)^4 \phi^2$$

$$- 1.985 \times 10^4 \left(\frac{R}{R_o} \right)^6 \phi^2$$

$$MPE = 14.37\%$$

$$APE = 2.28\%$$

(b) Blade Height = 0.125 inch

$$K = -2.511 + 0.49 \left(\frac{R}{R_o} \right)^2 + 103.4 \phi - 726.9 \phi^2 + 0.26 \left(\frac{T}{S} \right)$$

$$- 55.0 \left(\frac{R}{R_o} \right)^2 \phi + 405.0 \left(\frac{R}{R_o} \right)^4 \phi^2 + 0.045 \phi^{-1.0} - 2.6 \times 10^{-4} \phi^{-2}$$

$$+ 0.069 \left(\frac{R}{R_o} \right)^{-1.0} \quad (IV-8)$$

$$MPE = 11.92\%$$

$$APE = 2.11\%$$

Figure IV-3 shows a plot of the regression equation for the bladed disk in water. This equation, which reflects the change in vortex mode with radius and the dependency of K on T and T/S, is applicable to both outward and inward flow conditions. Flow coefficient, within the range tested, had no measurable effect on K value. The effect on K of reducing the number of blades from 24 to 12 or 6 is relatively small. This effect is consistent with results reported by other investigators such as Stepanoff and Acosta.

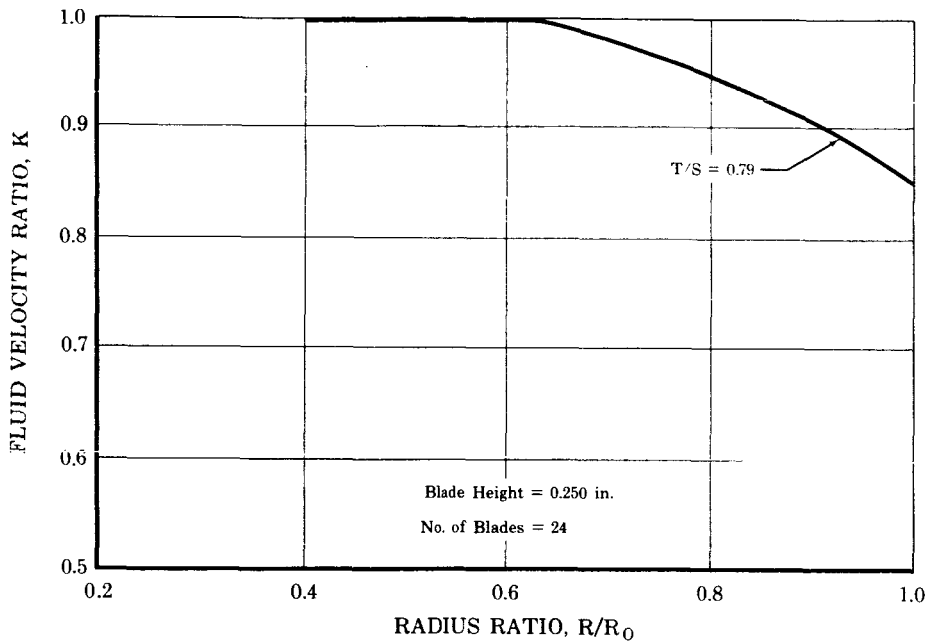
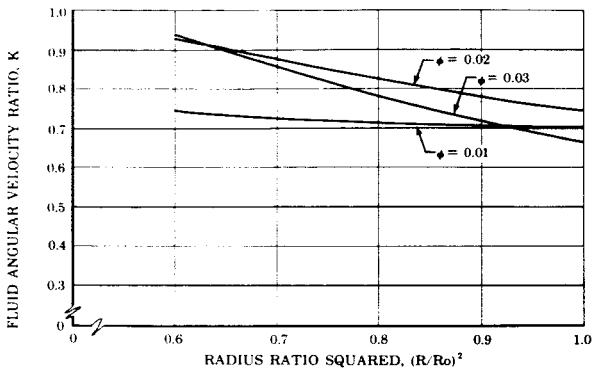


Figure IV-3. Fluid Angular Velocity Correlation FD 7833A for 24-Blade, 0.250-in. Impeller in Water, Inward and Outward Flow

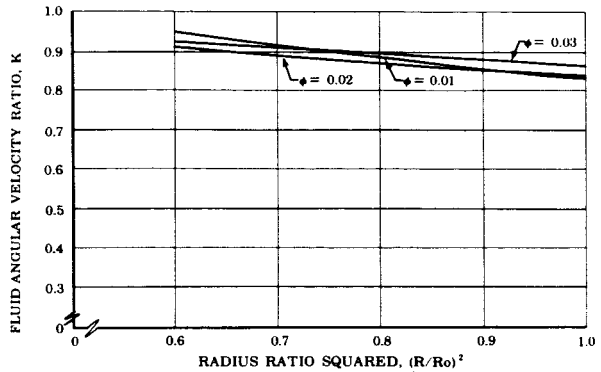
Figure IV-4 provides plots of K vs radius ratio squared at three values of T/S (0.8, 0.6, and 0.4) for the two blade heights (0.125 and 0.250 inch) for radially inward flow with liquid hydrogen. The reduction in the number of blades from 24 to 12 or 6 had no measurable effect on K for either outward or inward flow.

3. Smooth Disk, Bladed Housing

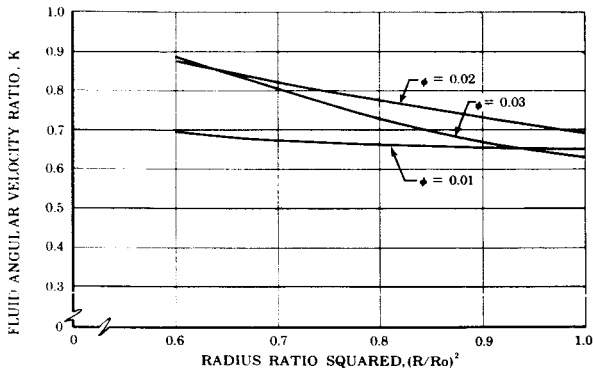
Within the range of variables tested there was no measurable change in pressure for either inward or outward flow so that K for this case is equal to zero.



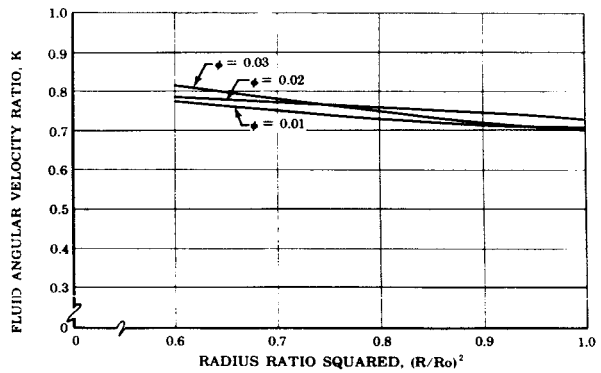
(a) $T = 0.125$ in.,
 $T/S = 0.8$



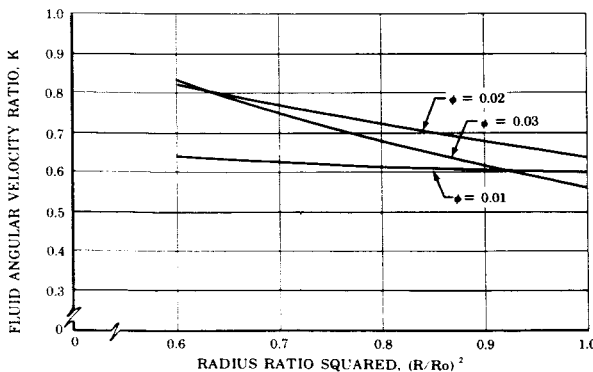
(d) $T = 0.250$ in.,
 $T/S = 0.8$



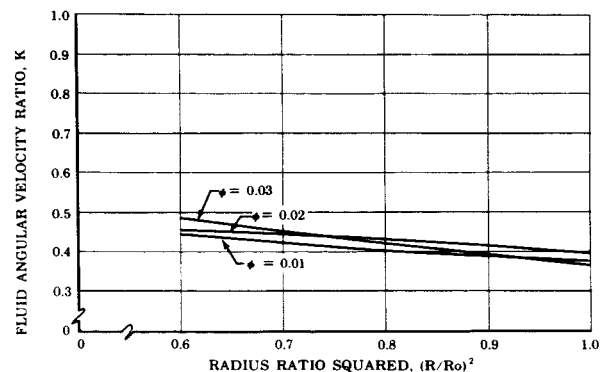
(b) $T = 0.125$ in.,
 $T/S = 0.6$



(e) $T = 0.250$ in.,
 $T/S = 0.6$



(c) $T = 0.125$ in.,
 $T/S = 0.4$



(f) $T = 0.250$ in.,
 $T/S = 0.4$

Figure IV-4. Fluid Velocity Ratio vs Radius Ratio Squared for Bladed Disk in Liquid Hydrogen, Radially Inward Flow

FD 11003B

4. Inlet and Discharge Geometry

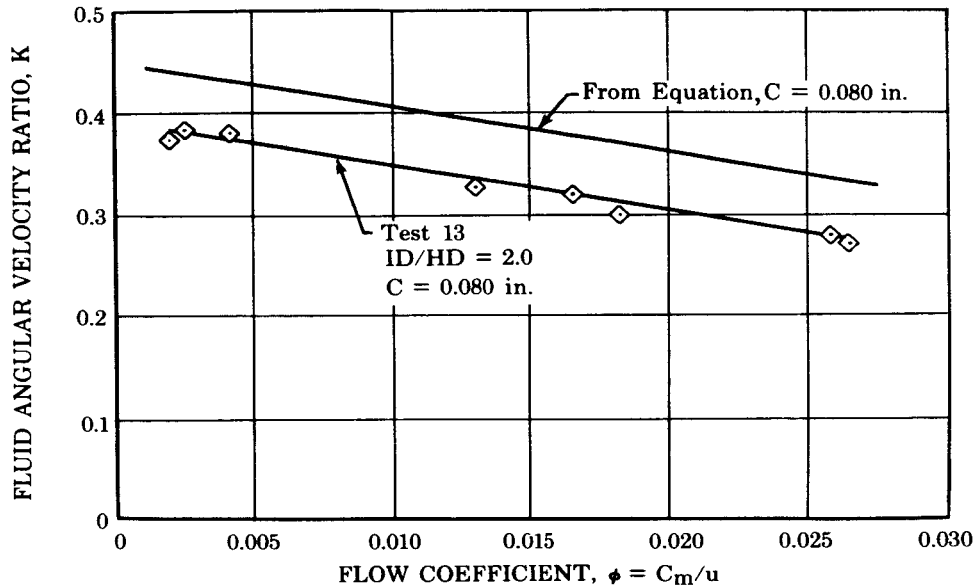
The effect on K of changes to the inlet and discharge geometry was investigated in Phases II and III. The effects of these changes are discussed in the following paragraphs.

a. Inlet Hub

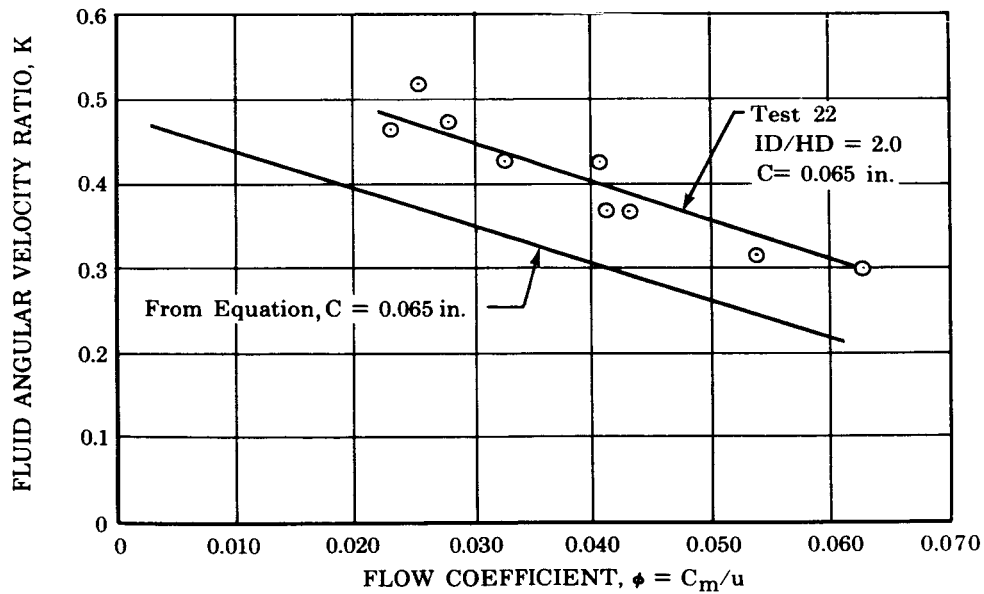
As discussed in Section III, the addition of an inlet hub to the smooth disk with a smooth housing had a significant effect on head rise in both water and hydrogen. This effect on the value of K is depicted in figure IV-5 for both water and hydrogen. These curves show a decrease in K for water and an increase in K for hydrogen with the addition of an inlet hub with an inlet-to-hub diameter ratio (ID/HD) of 2. Tests with a larger diameter hub ($ID/HD = 1.33$) produced the same results. An explanation of the differences in the two fluids and/or the effect of the hub in either case would require a detailed investigation of the flow conditions including turbulence and recirculation in both configurations. Due to the inconclusive data on the inlet hub effects in Phase III, as discussed in Section III, and because the Phase II tests were conducted at only one disk-to-housing clearance, it is not known if the magnitude of the inlet hub effect is the same at all clearances. For this reason the equation for K for the smooth disk has not been modified to include the inlet hub case.

b. Tip Blockage, Bladed Disk

The addition of blockage rings at the tip of the bladed disk to simulate housing overhang had no measurable effect on fluid velocity in liquid hydrogen. However, in water, the tip blockage changed the vortex mode creating a forced vortex and making K a constant with radius as shown in figure IV-6. This effect was noted in tip clearances (Z) from 0.050 to 0.150 in. with the 0.125-inch high blades at a blade-to-housing clearance of 0.065 inch. It is possible that this effect would be reduced at tip clearances greater than S (the sum of blade height and blade-to-housing clearance, in this case, 0.190 in.). However, for cases within the Z/S ratios tested (0.26 to 0.79), it appears that the (R/R_0) term in the equation for K may be replaced with a constant equal to 0.170.



(a) For Water



(b) For Liquid Hydrogen

Figure IV-5. Fluid Velocity Ratio vs Flow Coefficient FD 10981A for Smooth Disk with Inlet Hub, Radially Outward Flow

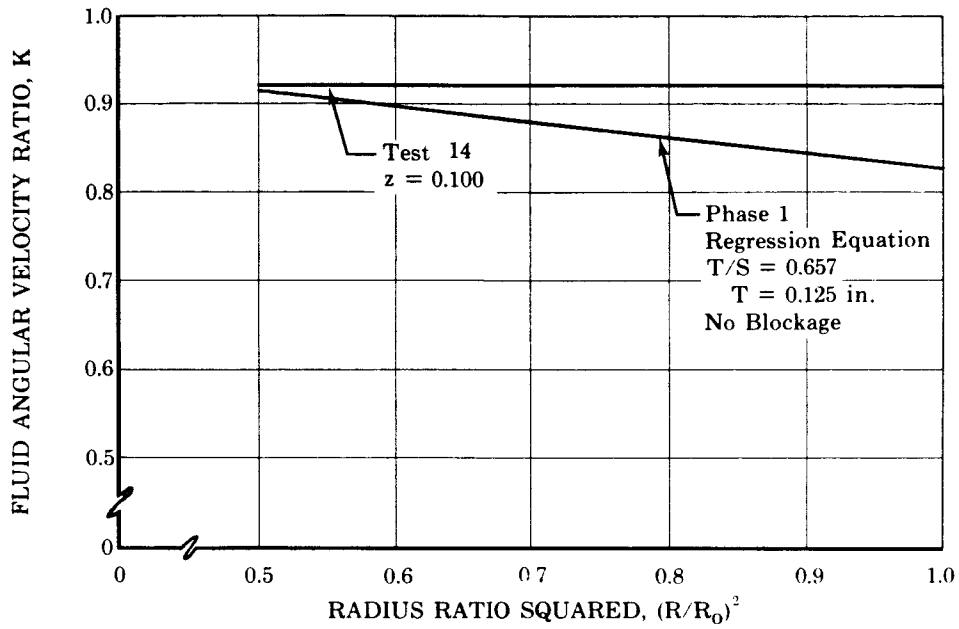


Figure IV-6. Fluid Velocity Ratio vs Radius Ratio Squared for Bladed Disk with Tip Blockage in Water, Radially Outward Flow

SECTION V
DISCUSSION OF RESULTS

A. GENERAL

The results of the experimental program have yielded an empirical method for predicting the radial pressure distribution generated by low-flow bladed or smooth (unbladed) disks in smooth housings and bladed housings with smooth disks within the range of variables tested.

The equations for K derived from the water tests are considered applicable to incompressible fluids at disk Reynolds numbers greater than 10^6 , while the equations derived for liquid hydrogen are applicable only to liquid hydrogen because of the unique properties of this fluid, such as the variation of density and specific heat with temperature.

The equations for K are considered valid for application to the prediction of radial pressure distribution within the range of variables tested, as given in table V-1. Their use outside these ranges should be with caution.

The results discussed in Sections III and IV have been concerned with the prediction of head distribution or pressure distribution with no appreciable density change. In an actual case the density may vary enough to have an effect on the pressure distribution. The major cause of the density change is attributed to an increase in fluid temperature due to fluid friction and turbulence. Figure V-1 will serve to demonstrate the magnitude of the temperature change observed during testing.

From the water test data it was observed that a small temperature rise (maximum 9°F) occurred for the outward flow condition and a negligible temperature change occurred with inward flow. This would have a negligible effect on density and hence pressure distribution.

In liquid hydrogen there was a temperature rise with outward flow on both the smooth and bladed disks. However, the inward flow temperature data was inconsistent. In the low pressure (95 psia) tests, the temperature for inward flow was nearly constant but in the test at high pressure (650 psia) there was a significant increase in temperature (5° to 10°F). In the high-pressure test the temperature rise on the front face (outward flow condition) was nearly the same as in the low-pressure tests.

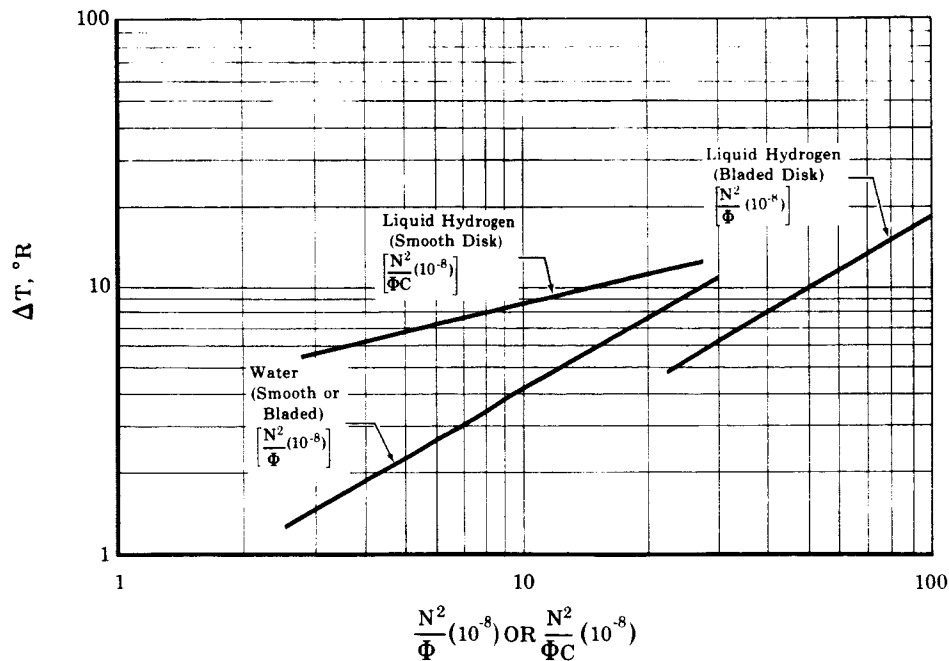


Figure V-1. Temperature Rise for Outward Flow FD 14538

The difference in ΔT between the low-pressure and high-pressure tests can be attributed to the unique properties of hydrogen. The expansion of hydrogen to a lower pressure can result in a temperature increase or decrease depending on the initial properties (temperature and pressure) of the fluid. In addition, the specific heat of hydrogen varies radically with pressure as well as temperature, especially at lower temperatures (below $80^\circ R$) which was the region of primary interest in this study. As the specific heat changes, of course, the ΔT for a given heat input also changes. To make the pressure prediction analysis complete, empirically determined moment coefficients based on the observed data were incorporated to enable the prediction of temperature rise. This is then applied to the head rise calculation to yield the pressure distribution. A correlation was established from the data for both the smooth and bladed disk for both fluids. The temperature rise was found to be a function of ω^2/ϕ , specific heat, moment coefficient, and gap width, S .

The equations derived for these cases are incorporated in the computer program discussed in Appendix A.

Table V-1

Configuration & Test Fluid	ϕ	C, in	Re (10^6)
Smooth Disk			
Water	0-0.035	0.040-0.138	6.87-22.5
Hydrogen	0.004-0.123	0.024-0.138	77.2-123.0
Bladed Disk			
Water	0-0.024	0.020-0.125	3.8-27.9
Hydrogen	0.010-0.046	0.035-0.156	37.3-121.7

B. FORMULATION OF COMPUTER PROGRAM

To provide a complete and readily usable pressure prediction system a computer program has been formulated based on the equations for K developed from the experimental data. This program, which is written in Fortran II for use on the IBM 7090 computer, will provide head and pressure distribution and the axial force generated by this pressure distribution for any of the configurations included in the experimental investigation. The computer program, when supplied with inputs for a specific configuration and set of operating conditions, will perform the preliminary calculations required for various parameters, such as rotor speed, fluid velocity, density, specific heat, and viscosity. The K value is then calculated using the applicable equation from Section III and this K value (s) is then applied to the modified forced vortex equation to determine head rise.

A more detailed description of the formulation of the computer program is presented in Appendix A.

SECTION VI
CONCLUSIONS

Based on the results of the pressure prediction program for radial, low-flow impellers the following conclusions may be stated.

1. The water and liquid hydrogen tests revealed several major differences, the most significant of which follow:
 - a. Smooth Disk, Smooth Housing (outward flow) - (1) The change in fluid velocity ratio, K, with disk-to-housing clearance is linear in water and nonlinear in hydrogen; (2) The addition of an inlet hub reduced the K value in water and increased K in hydrogen.
 - b. Bladed Disk, Smooth Housing (outward flow) - K was determined to be constant and equal to unity for all cases tested in hydrogen but varied as a function of R/R_o , T/S, and T in water.
 - c. Smooth Disk, Bladed Housing (outward and inward flow) - There was no measurable pressure change over the disk radius so that K was zero for all values of clearance tested with both water and liquid hydrogen.
2. The fluid velocity ratio, K, and therefore the pressure distribution for the smooth disk with a smooth housing in hydrogen and water was determined to be dependent on flow coefficient and clearance for radially outward flow,
$$K = f(C, \phi)$$
and for the radially inward flow,
$$K = f(R/R_o, C, \phi)$$
3. For the bladed disk in hydrogen, K was determined to be independent of all variables within the ranges tested and equal to unity for radially outward flow. A reduction from 24 to 12 or 6 blades had no effect on K.

4. For the bladed disk with radially inward flow in hydrogen, K was determined to be dependent on flow coefficient, T, T/S, and R/R_o ,

$$K = f(\phi, T, T/S, R/R_o)$$

5. K values for the bladed disk in water were determined to be dependent on R/R_o , T/S, and T. One equation was found to fit both inward and outward flow conditions.

$$K = f(R/R_o, T/S, T)$$

6. Impeller tip blockage on the bladed disk in liquid hydrogen had no effect on K, which remained constant and equal to unity as it was without blockage; however, for water the tip blockage raised the value of K and made it independent of R/R_o .
7. The results of the smooth disk-smooth housing tests of Phase II, both in water and liquid hydrogen, do not agree with the findings of other investigators such as Daily and Nece (Reference 1), who have found that a zero or shutoff flow condition in the channel between a stationary housing and a smooth rotating disk the fluid velocity ratio K is approximately 0.5 for clearances below 0.200 in. The experience plus a scarcity of data resulted in the Phase I smooth disk test results being plotted (K vs ϕ) as a family of curves for varying clearance fanning out from a common apex at a K value of approximately 0.5. The water tests in Phase II gave indications that the lines of constant clearance do not converge at $K = 0.5$ but are actually parallel and that the slope of a curve of K vs clearance is quite steep. (See figure IV-1.) Subsequent tests in liquid hydrogen confirmed these results (figure IV-1).
8. The high-response pressure data from the bladed disk tests in liquid hydrogen failed to indicate the relationship between the pressure pulse across the blade and pressure, rotor speed, or flowrate. Therefore, it is not possible at this time to derive an equation for predicting blade loading. Further testing over a wider range of operating conditions might establish trends that would be useful in formulating an accurate prediction system for blade loading.

SECTION VII
REFERENCES

1. Daily, J.W. and R. E. Nece, "Chamber Dimension Effects on Induced Flow and Frictional Resistance of Enclosed Rotating Disks," ASME Transactions, Journal of Basic Engineering, March 1960, pp 217-232.
2. Schlichting, H., "Boundary Layer Theory," 4th Edition, McGraw-Hill Publishing Company, 1962.
3. Stepanoff, A. J. "Centrifugal and Axial-Flow Pumps, Wiley, New York, New York, 1948.
4. Acosta, A. J. "Experimental and Theoretical Investigations of Two-Dimensional Centrifugal Pump Impellers," ASME Transactions, Vol. 76, 1954.

APPENDIX A
PRESSURE PREDICTION FOR RADIAL FLOW IMPELLERS
FORTRAN PROGRAM FORMULATION
(PWA FRDC DECK NO. 5363)

The final task in the third phase of the pressure prediction program was to combine the results of the investigations on the various configurations into a Fortran program to be used with the IBM 7090 computer.

The purpose of the computer program is to calculate the radial head and pressure distributions for a prescribed set of operating conditions and geometry. It is important to note whether the prescribed conditions fall within the range of variables investigated in the experimental program because it is not known whether an extrapolation beyond the experimental range is valid.

The input required for this program consists of flowrate, rotor speed, clearance, blade height, blade thickness, number of blades, inlet temperature, inlet pressure, outer radius, inner radius, flow direction, the type of fluid (hydrogen or water), and whether the disk is bladed or smooth (unbladed).

The output includes station, radius, radius squared, head, pressure, and total thrust. The calculation consists of a numerical integration of the radial pressure rise equation beginning at the inlet radius if the flow is radially outward or the outer radius if the flow is inward. The calculation is performed at 12 stations along the disk at equal increments of radius squared. In the case of hydrogen, where a large variation of density and specific heat with temperature exists, calculations are iterated until convergence of pressures is obtained.

Because each of the configurations have a unique equation for K, separate routines are required for each case as specified by the input.

The program begins by specifying the input conditions as follows:

Flow = Inward or outward

Fluid = Water or liquid hydrogen

Configuration = Outward flow

1. Smooth disk - water
2. Bladed disk - water

3. Smooth disk - LH₂

4. Bladed disk - LH₂

Configuration = Inward flow

1. Smooth disk - water

2. Bladed disk - water

3. Smooth disk - LH₂

4. 0.125-inch bladed disk - LH₂

5. 0.250-inch bladed disk - LH₂

Q = Flowrate - gpm

RPM = Rotational speed

CL = Clearance - inches

BH = Blade height - inches

BT = Blade thickness - inches

BN = Number of blades

TI = Inlet static temperature - °F

RO = Outer radius - inches

RI = Inner radius - inches

PI = Inlet static pressure - psi

Calculations which remain the same for each case are:

1. The flow passage gap height

$$S = BH + CL$$

2. The meridional flow area at the disk outer radius

$$AT = \left[2 \pi RO (BH + CL) - (BH)(BT)(BN) \right] / 144$$

3. Disk angular velocity

$$\omega = \pi (RPM) / 30$$

4. Tangential velocity of disk at RO

$$u = \omega RO / 12$$

5. Radius squared increment

$$drs = (R_o^2 - R_1^2) / 12$$

Fluid properties at the inlet of the disk

6. Fluid density determined by:

$$\gamma_i = 63.218 - 0.0128 (T_i), \text{ for water}$$

(accurate within 2% between 60 and 150°F)

or

$$\gamma_i = f(P_i, T_i), \text{ for liquid hydrogen}$$

(This density subroutine is taken from the latest available P-V-T relationships for para-hydrogen from NBS.)

7. Fluid specific heat determined by:

$$C_{pi} = 1.0, \text{ for water}$$

or

$$C_{pi} = f(P_i, T_i), \text{ for liquid hydrogen}$$

8. Fluid Viscosity determined by;

$$\mu_i = 8.084 \times 10^{-4} (T_i)^{-1.02177}, \text{ for water}$$

(accurate to within 2% between 60 and 150°F)

or

$$\mu_i = f(P_i, T_i), \text{ for liquid hydrogen}$$

The inlet head is calculated as,

$$H_i = P_i(144)/\gamma_i$$

For the initial calculation the flow coefficient is based on the volumetric flowrate at the inlet;

$$\phi = Q/(448.8 \times A_t \times u)$$

For the outward flow case the specified inlet pressure and inlet temperature are used for the fluid conditions at the inner radius, which is the first station.

$$P_1 = P_i$$

$$T_1 = T_i$$

$$RS_1 = (R_i)^2$$

$$\gamma_1 = \gamma_i$$

$$H_1 = H_i$$

$$C_{p1} = C_{pi}$$

$$\mu_1 = \mu_i$$

The numerical integration is begun by entering into a loop which repeats the calculations for head and pressure at each radial station from the inlet to the outer radius of the disk.

For each incremental step from $I = 1$ to 12

$$RS(I + 1) = RS(I) + DRS$$

At station 1, the inlet

$$RS(1) = RS(I)$$

For $I = 1$

$$RS(2) = RS(I) + DRS$$

Calculations of K are made at the midpoint of each radial increment given by,

$$RB = \left[(RS_2)^{\frac{1}{2}} + (RS_1)^{\frac{1}{2}} \right] / 2$$

The temperature rise in the fluid caused by friction and turbulence losses is predicted by equating the energy input calculated by

$$E = T\omega = C_M \left(\frac{1}{g}\right) \frac{\gamma}{g} \omega^3 (R_2^5 - R_i^5)$$

to the enthalpy increase in the fluid given by

$$Q = \dot{m} C_p \Delta T$$

The combination yields the equation for calculating the approximate overall temperature rise in the fluid

$$T = \frac{C_M R_o^3 (\omega^2)}{2 (10^5) C_p (S\phi)}$$

Since this equation is approximate, the value of C_M was determined experimentally from the temperature data obtained in the test program. The values determined for hydrogen were approximately the values expected based on comparisons with the data from previous investigations with water. The following values of C_M are recommended for use in this program for the specific configurations.

Fluid	Configuration	C_M
LH ₂	smooth disk	0.003
LH ₂	bladed disk	0.020
Water	smooth disk	0.003
Water	bladed disk	0.025

For the purpose of the step-by-step calculation along the disk radius, the temperature rise is assumed to vary linearly with the radius squared so that,

$$T(I = 1) = T(I) + \Delta T/12$$

The input statement determines which equation is to be used for the calculation of K.

$$K = \text{as given in Section IV for the various configurations}$$

The head rise is calculated for the increment from R_1 to R_2 as

$$\Delta H = K^2 \omega^2 (R_2^2 - R_1^2) / (288.0 \times 32.2)$$

The head at station 2 is calculated as,

$$H_2 = H_1 + \Delta H$$

Iteration on pressure:

The pressure at station 2 is calculated as,

$$P_2^1 = H_2 \gamma_1 / 144$$

γ_2 is found based on P_2^1 from the density equations previously written. A new P_2 is calculated based on the value of γ_2 as,

$$P_2 = H_2 \gamma_2 / 144$$

P_2 is compared with P_2^1 ; if they agree within 1% the calculation continues, if not an iteration is performed until convergence is achieved.

The thrust on the area between R_1 and R_2 is calculated as,

$$F(I) = \frac{P(I) + P(I + 1)}{2} \left(RS(I + 1) - RS(I) \right)$$

and summation is taken over the disk

$$FT = FT + F(I)$$

The calculations are complete for the first increment of radius. The program now repeats the procedure by indexing to the $RS(I + 1)$ statement and proceeding with $I = 2$. The initial values taken for $I = 2$ are those previously calculated at $I = 1$. This procedure is continued until $I = 12$ where R is equal to the outer disk radius.

The calculation procedure for inward flow is identical to that of outward flow except that the calculation begins at the outer radius and proceeds to the inner radius. The inlet conditions are referred to the disk outer radius.

The following is a listing of the source deck for the computer program. The listing presents the information contained on each card in the basic program. The subroutines for fluid properties, i.e., density, specific heat, and viscosity are not included. A notation appears in the listing wherever the property subroutines are used. Included at the end of the listing is an input instruction sheet which provides the format to be used for each case.

Pressure Prediction Computer Program Source Deck Listing
(PWA FRDC Deck No. 5363)

```

*          FORTRAN
*          PRESSURE PREDICTION FOR RADIAL FLOW IMPELLERS
          DIMENSION TITLE(12) , T(15) , P(15) , H(15) , R(15) , F(15) , RHO(
115) , RAD(15)
10 READ 20,(TITLE(I) , I=1 ,12)
20 FORMAT (12A6 )
   READ 30,FLOW,CONF, FLUID, Q, RPM, CL, BH,BT
30 FORMAT(8F10.4)
   READ 40,BN, TI, RO, RI, PIN,CMP
40 FORMAT(6F10.4)
   ICONF= CONF
   PI= 3.1416
   S= BH+ CL
   AT= ( PI* 2.0 * RO*(BH+CL) - BH*BT* BN) / 144.0
   OMEGA= PI/30.0 * RPM
   U= OMEGA* RO/ 12.0
   DR= (RO**2 - RI**2 ) / 12.0
   IF(FLUID- 1.0)60,50, 60
50 TI= TI- 460.0
   RHOI= 63.218 - 0.0128 * TI
   CPI= 1.0
   VIS= 8.084E-04 / TI**1.02177
   RE1= OMEGA* RO**2 / (144.0 * VIS)
   GO TO 70
60 RHOI= DENST( TI, PIN*144.0)
   CALL VCPA( PIN,TI, CPI)
   CPI= CPI/778.26
   CALL VISCO(RHOI,TI, VIS)
   RE1= OMEGA* RO**2 * RHOI/ VIS/ 144.0
70 HI = PIN/RHOI* 144.0
   IF( FLOW- 1.0 )320,320, 80
C
C          OUTWARD FLOW
C
80 FT= 0.0
   T(1) = TI
   P(1) = PIN
   H(1) = HI
   R(1) = RI**2
   RHO(1) = RHOI
   DO 310 I=1 , 12
   R(I+1) = R(I) + DR
   RB= (SQRTF(R(I)) + SQRTF(R(I+1))) / 2.0
   GO TO( 90, 120, 150, 200, 290, 300),ICONF
90 CM= Q/(7.48 *60.0 * AT)
   PHI= CM/ U
   DTT= CMP* RO**3*OMEGA**2/(288.*1.0E+05*CPI* S*PHI*3.14159 )/12.
   XK= 0.578 - 4.11* PHI- 1.67 * CL
   IF(XK- 1.0)110,110, 100
100 XK= 1.0
110 CONTINUE
   GO TO 280
120 CM= Q/( 7.48 * 60.0 * AT)
   PHI= CM/ U
   DTT= CMP* RO**3*OMEGA**2/(288.*1.0E+05*CPI* S*PHI*3.14159 )/12.

```

Pressure Prediction Computer Program Source Deck Listing
(PWA FRDC Deck No. 5363) (Continued)

```

      XK= 0.951 - 0.282 (RB/RO) + 0.2137* (BH/S) + (0.175 *BH)      0056
      IF(XK- 1.0)140,140, 130      57
130  XK= 1.0      58
140  CONTINUE      59
      GO TO 280      60
150  CM= Q/ (7.48 * 60.0 * AT) * RHOI/ RHO(I)      61
      PHI= CM/ U      62
      IF(I-1) 160,160, 170      63
160  DTT= CMP* RO**3*OMEGA**2/(288.*1.0F+05*CPI* S*PHI*3.14159 )/12.      0064
170  CR= CL/ RO      65
      XK= 0.906 + 0.012 * PHI/CR- 5.36* PHI-(51.1 - 1295.3*CR)*CR      0066
      IF(XK- 1.0)190,190, 180      67
180  XK= 1.0      68
190  CONTINUE      69
      DELH= XK**2 * OMEGA**2 * (R(I+1) - R(I))/(288.0 * 32.2)      0070
      GO TO 230      71
200  PHI= Q*(RHOI/ RHO(I) ) / ( AT* U* 7.48 * 60.0 )      0072
C      73
      IF(I-1) 210,210, 220      74
210  DTT= CMP* RO**3*OMEGA**2/(288.*1.0E+05*CPI* S*PHI*3.14159 )/12.      0075
220  DELH= OMEGA**2 * (R(I+1) - R(I)) / (288.0 * 32.2)      0076
230  T(I+1) = T(I) + DTT      77
      H(I+1) = H(I) + DELH      78
      PFG= H(I+1) * RHO(I) /144.0      79
C      80
C      ITERATION ON PRESSURE      81
      KOUNT= 0      82
240  RHO(I+1) = DENST(T(I+1),PFG*144.0)      83
      P(I+1) = H(I+1) * RHO(I+1) /144.0      84
      IF (KOUNT)250,250, 260      85
250  D1= PFG- P(I+1)      86
      P11= PFG      87
      PFG= P(I+1)      88
      KOUNT= KOUNT+ 1      89
      GO TO 240      90
260  D2= PFG- P(I+1)      91
270  F(I)=(P(I) + P(I+1)) * PI* (R(I+1)- R(I))/ 2.0      92
      FT= FT+ F(I)      93
      GO TO 310      94
280  DELH= XK**2 * OMEGA**2 (R(I+1) - R(I) ) / (288.0 * 32.2)      0095
      H(I+1) = H(I) + DELH      96
      P(I+1) = H(I+1) * RHOI/ 144.0      97
      F(I) = (P(I)+ P(I+1))* PI*(R(I+1)- R(I)) / 2.0      0 98
      FT= FT+ F(I)      99
      T(I+1) =T(I)+ DTT      100
      RHOI= 63.216 - 0.0128 * T(I+1)      101
      GO TO 310      102
C      103
C      2000 AND 3000 ARE SAVED FOR BLADED HOUSING      0104
C      105
290  CONTINUE      106
300  CONTINUE      107
310  CONTINUE      108
      GO TO 470      109
320  FT= 0.0      110

```

Pressure Prediction Computer Program Source Deck Listing
(PWA FRDC Deck No. 5363) (Continued)

```

T(13)=TI 111
P(13) = PIN 112
H(13) = HI 113
R(13) = RO**2 114
RHO(13) = RHOI 115
C 116
C INWARD FLOW 117
C 118
DO 460 J=1,12 119
I= 14 - J 120
R(I-1) = R(I) - DR 121
RB= (SQRTF(R(I)) + SQRTF(R(I-1))) / 2.0 122
GO TO (350,360,370,380,440,330,340),ICONF 0123
C 124
C 4000 AND 5000 ARE SAVED FOR BLADED HOUSING 0125
C 126
330 CONTINUE 127
340 CONTINUE 128
350 CM= Q/ (7.48 * 60.0 * AT) 129
PHI= CM/ U 130
DTT= CMP* RO**3*OMEGA**2/(288.*1.0E+05*CPI* S*PHI*3.14159 )/12. 0131
CR= CL/ RO 132
RBO= RB/RO 133
XK= 0.3865 + 95.3 * PHI**2 -12.6*PHI*( RBO)**2 - 9.17E05* PHI* CR* 0134
1*3 + 27.8 * ( RBO)**2 *CR- 2.75E03*(RBO)**4 * CR**2 + 6.51E04* RBO 0135
2**6 * CR**3 + 2.13 * SQRTF(PHI) - 6.59 * CR 0136
GO TO 450 137
360 CM= Q/ (7.48 * 60.0 * AT) 138
PHI= CM/ U 139
DTT= CMP* RO**3*OMEGA**2/(288.*1.0E+05*CPI* S*PHI*3.14159 )/12. 0140
XK= 0.951 - 0.282 * (RB/RO) + (0.2137)*(BH/ S) + 0.175 *BH 0141
GO TO 450 142
370 CM= Q/ (7.48 * 60.0 * AT) 143
PHI= CM/U 144
DTT= CMP* RO**3*OMEGA**2/(288.*1.0E+05*CPI* S*PHI*3.14159 )/12. 0145
XK= 0.18 * PHI**0.16 /((RB/ RO)**1.434 * CL**0.233) 0146
GO TO 390 147
380 CM= Q/ (7.48 * 60.0 * AT) 148
PHI= CM/U 149
DTT= CMP* RO**3*OMEGA**2/(288.*1.0E+05*CPI* S*PHI*3.14159 )/12. 0150
CR= CL/ RO 151
TS= BH/ S 152
RBO= RB/RO 153
XK= -2.511 + 0.49*RBO**2 + 103.4*PHI- 726.9* PHI**2 +0.26*TS- 55.0 0154
1 * RBO**2 * PHI+ 405.0* RBO**4 * PHI**2 + 0.045 /PHI- 2.6E-04 /PHI 0155
2**2 + 0.069 / RBO 156
390 DELH= XK**2 * OMEGA**2 * (R(I) - R(I-1)) / (64.4 * 144.0 ) 0157
T(I-1) = T(I) + DTT 158
H(I-1) = H(I) - DFLH 159
PFG= H(I-1) * RHO(I) / 144.0 160
C 161
C ITERATE ON PRESSURE 162
C 163
KOUNT= 0 164
400 RHO(I-1) = DENST(T(I-1),PFG*144.0 ) 165

```

Pressure Prediction Computer Program Source Deck Listing
(PWA FRDC Deck No. 5363) (Continued)

```

P(I-1) = H(I-1) * RHO(I-1) / 144.0
IF(KOUNT) 410,410, 420
410 D1= PFG- P(I-1)
P11= PFG
PFG= P(I-1)
KOUNT= KOUNT+ 1
GO TO 400
420 D2= PFG- P(I-1)
430 F(I-1) = (P(I-1) + P(I)) * (R(I) - R(I-1))* PI/ 2.0
FT= F(I-1) + FT
GO TO 460
440 CM= Q/ (7.48 * 60.0 * AT)
PHI= CM/ U
DTT= CMP* RO**3*OMEGA**2/(288.*1.0E+05*CPI* S*PHI*3.14159 )/12.
TS= BH/ S
RBO= RB/RO
XK=-0.8819 + 1.24 * RBO**2 - 1.943*RBO**4 +.84100 *RBO**6 + 4.06 *
1 TS- 2.41 *(TS)**2 - 23.94 *RBO**2 * PHI+ 1283.1*RBO**4 * PHI**2 -
2 1.985E04* RBO**6 * PHI**3
GO TO 390
450 DELH= XK**2 * OMEGA**2 * (R(I) - R(I-1)) / (288.0 * 32.2)
H(I-1) = H(I) - DELH
P(I-1) = H(I-1)* RHOI/144.0
F(I-1) = (P(I-1) + P(I)) * (R(I) - R(I-1))* PI/ 2.0
T(I-1) = T(I) + DTT
RHOI= 63.216 - 0.0128 * T(I-1)
FT= F(I-1) + FT
460 CONTINUE
470 PRINT 520
IF(FLUID- 1.0)500,480, 500
480 TI= TI+ 460.0
DO 490 I=1,13
490 T(I) = T(I) + 460.0
500 PRINT 510, (TITLE(I),I=1,12)
510 FORMAT( //,10X,12A6 )
520 FORMAT( 1H1, //, 32X , 46H PRESSURE PREDICTION FOR RADIAL FLOW
1IMPELLERS)
IF(FLOW- 1.0)530,530, 610
530 GO TO(540,550,560,570,580,590,600),ICONF
540 PRINT 750
GO TO 680
550 PRINT 760
GO TO 680
560 PRINT 770
GO TO 680
570 PRINT 780
GO TO 680
580 PRINT 790
GO TO 680
590 PRINT 800
GO TO 680
600 PRINT 810
GO TO 680
610 GO TO (620,630,640,650,660, 670),ICONF
620 PRINT 820

```

Pressure Prediction Computer Program Source Deck Listing
(PWA FRDC Deck No. 5363) (Continued)

```

        GO TO 680                                221
630 PRINT 830                                    222
        GO TO 680                                223
640 PRINT 840                                    224
        GO TO 680                                225
650 PRINT 850                                    226
        GO TO 680                                227
660 PRINT 860                                    228
        GO TO 680                                229
670 PRINT 870                                    230
        GO TO 680                                231
680 PRINT 690, Q,RPM,CL,BH,BT,BN,TI,RO,RI,PIN    0232
690 FORMAT(///12H FLOW RATE =,18X,F10.4,1X,3HGPM,/14H WHEEL SPEED =, 0233
        116X,F10.2,1X,3HRPM,/,12H CLFARANCE =,18X,F10.4,1X,2HIN,/, 0234
        215H BLADE HEIGHT =,15X,F10.4,1X,2HIN,/,18H BLADE THICKNESS =,12X, 0235
        3 F10.4,1X, 2HIN, / 236
        419H NUMBER OF BLADES =,11X,F10.4,/ ,20H INLET TEMPERATURE =,10X, 0237
        5 F10.4,1X, 9HDEGRFFS R,/, 15H OUTER RADIUS =,15X,F10.4,1X,2HIN, /, 0238
        6 15H INNER RADIUS =,15X,F10.4,1X,2HIN,/,17H INLET PRESSURE =,13X, 0239
        7 F10.4,1X,3HPSI, /// ) 240
        PRINT 700, PHI 241
700 FORMAT( 19H FLOW COEFFICIENT =,11X,F10.4) 0242
        PRINT 710, RE1 243
710 FORMAT( 19H REYNOLDS NUMBER ,11X,E10.4/) 0244
        DO 720 I= 1,13 245
720 RAD(I) = SQRTF(R(I) ) 246
        PRINT 740,(I,RAD(I),R(I),H(I) ,P(I) , T(I),I=1, 13) 0247
        PRINT 730, FT 248
730 FORMAT( /// 15H TOTAL THRUST =,15X,E10.4 ,1X,3HLBS ) 0249
        GO TO 10 250
740 FORMAT(7X,7HSTATION, 15X ,6HRADIUS, 8X,14HRADIUS SQUARED,11X,4HHEA 0251
        1D,14X,8HPRESSURE,12X,11HTEMPERATURE / 252
        2 ,29X,6HINCHES, 9X,13HSQUARE INCHES,11X,4HFEET, 0253
        316X,3HPSI,15X, 9HDEGREES R , 254
        4 // (10X,12,14X,F10.3,10X,F10.3,10X,F10.3,10X,F10.3)) 0255
750 FORMAT( 54H THIS CASE IS INWARD FLOW , SMOOTH DISK , AND WATER ) 0256
760 FORMAT( 54H THIS CASE IS INWARD FLOW , BLADED DISK , AND WATER ) 0257
770 FORMAT( 54H THIS CASE IS INWARD FLOW , SMCOTH DISK , AND HYDROGEN) 0258
780 FORMAT( 54H THIS CASE IS INWARD FLOW , 0.125 BLADED, AND HYDROGEN) 0259
790 FORMAT( 54H THIS CASE IS INWARD FLOW , 0.250 BLADED, AND HYDROGEN) 0260
800 FORMAT( 54H THIS CASE IS INWARD FLOW , BLADED HSG , AND WATER ) 0261
810 FORMAT( 54H THIS CASE IS INWARD FLOW , BLADED HSG , AND HYDROGEN) 0262
820 FORMAT(55H THIS CASE IS OUTWARD FLOW , SMOOTH DISK , AND WATER ) 0263
830 FORMAT(55H THIS CASE IS OUTWARD FLOW , BLADED DISK , AND WATER ) 0264
840 FORMAT(55H THIS CASE IS OUTWARD FLOW , SMOOTH DISK , AND HYDROGEN) 0265
850 FORMAT(55H THIS CASE IS OUTWARD FLOW , BLADED DISK , AND HYDROGEN) 0266
860 FORMAT(55H THIS CASE IS OUTWARD FLOW , BLADED HSG , AND WATER ) 0267
870 FORMAT(55H THIS CASE IS OUTWARD FLOW , BLADED HSG , AND HYDROGEN) 0268
        END 269

```

Pressure Prediction Computer Program Input Instruction Sheet
(PWA FRDC Deck No. 5363)

TITLE CARD ANY DESIRED COMMENTS 2-72

NOTE VARIABLES ARE INPUT IN FIELDS OF TEN. ALL VARIABLES MUST
HAVE A DECIMAL POINT.

CC	10	20	30	40	50	60	70	
	BN	TI	RO	RI	PI	CMP		

FLOW CONF FLUID Q RPM CL BH BT

FLUID = 1.0 FLUID IS H2O
 = 2.0 FLUID IS LH2

FLOW = 1.0 FLOW IS INWARD
 = 2.0 FLOW IS OUTWARD

CONF FOR OUTWARD FLOW
 = 1.0 SMOOTH DISK , WATER
 = 2.0 BLADED DISK , WATER
 = 3.0 SMOOTH DISK , LH2
 = 4.0 BLADED DISK , LH2

CONF FOR INWARD FLOW
 = 1.0 SMOOTH DISK , WATER
 = 2.0 BLADED DISK , WATER
 = 3.0 SMOOTH DISK , LH2
 = 4.0 0.125 BLADED DISK , LH2 FLOW
 = 5.0 0.250 BLADED DISK , LH2 FLOW

Q = FLOW RATE - GPM
 RPM = REVOLUTIONS PER MINUTE
 CL = CLEARANCE - INCHES
 BH = BLADE HEIGHT - INCHES
 BT = BLADE THICKNESS - INCHES
 BN = NUMBER OF BLADES
 TI = INLET STATIC TEMPERATURE - DEGREES RANKINE
 RO = OUTER RADIUS - INCHES
 RI = INNER RADIUS - INCHES
 PI = INLET STATIC PRESSURE - PSI
 CMP = MOMENT COEFFICIENT - NO DIMENSIONS